12-2007

Electroanalysis of Metals in Biological and Environmental Samples at Bismuth Electrodes

Kristie Carter Armstrong
University of Tennessee - Knoxville

To the Graduate Council:

I am submitting herewith a dissertation written by Kristie Carter Armstrong entitled "Electroanalysis of Metals in Biological and Environmental Samples at Bismuth Electrodes." I have examined the final electronic copy of this dissertation for form and content and recommend that it be accepted in partial fulfillment of the requirements for the degree of Doctor of Philosophy, with a major in Chemistry.

Ziling Xue, Major Professor

We have read this dissertation and recommend its acceptance:

James Q. Chambers, Michael J. Sepaniak, Svetlana Zivanovic

Accepted for the Council:

Carolyn R. Hodges

Vice Provost and Dean of the Graduate School

(Original signatures are on file with official student records.)

To the Graduate Council:

I am submitting herewith a dissertation written by Kristie Carter Armstrong entitled “Electroanalysis of Metals in Biological and Environmental Samples at Bismuth Electrodes.” I have examined the final electronic copy of this dissertation for form and content and recommend that it be accepted in partial fulfillment of the requirements for the degree of Doctor of Philosophy, with a major in Chemistry.

Ziling Xue, Major Professor

We have read this thesis
and recommend its acceptance:

James Q. Chambers

Michael J. Sepaniak

Svetlana Zivanovic

Accepted for the Council:

Carolyn R. Hodges, Vice Provost and
Dean of the Graduate School

(Original signatures are on file with official student records.)

ELECTROANALYSIS OF METALS IN BIOLOGICAL AND ENVIRONMENTAL SAMPLES AT BISMUTH ELECTRODES

A Dissertation Presented for

the Doctor of Philosophy Degree

The University of Tennessee, Knoxville

Kristie Carter Armstrong

December 2007

DEDICATION

This dissertation is dedicated to Mom, Dad, Mamaw, and Sid for walking beside me along this path, and to Will for holding my hand through this journey.

I can do all things through Him who gives me strength.

Philippians 4:13

ACKNOWLEDGEMENTS

There are many who have been instrumental in my accomplishments. First and foremost I thank my God; faith and grace are my foundation. Special thanks to my advisor, Dr. Xue, for being my mentor and teacher. His guidance and encouragement were essential to my graduate studies. He was compassionate to and supportive of me during some difficult times. I have great appreciation for Dr. James Chambers for taking time out of his retirement to guide with me on my electrochemical experiments. It was an honor to get to know Dr. Chambers beyond the classroom, and to be able to talk to him about his golfing trips and dogs. Thanks also to my other committee members, Drs. Michael Sepaniak and Svetlana Zivanovic, for taking the time and consideration to participate in such an important part in my life.

Many people in the chemistry department have helped me in one way or another. Art Pratt is a talented glassblower, and without him, the making of my bismuth electrode would have been impossible. Gary Wynn designed and built the multi-sample photochemical reactor. He has great expertise in the area of electronics, and his patience with me during the process is greatly appreciated. I cannot say thank you enough to Bill Gurley for helping me so many times with so many things at a moment's notice. Thanks to Johnny Jones also for his willingness to help with all of my computer glitches and email woes. I would like to thank my professors, Drs. Michael Sepaniak, Georges Guiochon, James Chambers, Ziling (Ben) Xue, and Charles Feigerle for teaching me a subject

which they are so passionate about. Other faculty and staff who have been of great help are Dr. Fred Schell, Dr. Craig Barnes, Dr. Jim Green, Dr. Jeffery Kovac, Dr. Rose Boll, Dr. Gerald Nyssen, Dr. Al Hazari, Dr. George Schweitzer, Dr. Jamie Adcock, Tray Allen, Sharon Marshall, Melissa Walker, Gail Cox, Darrel Lay, Pat Kerschieter, Kathy Haggerty, Lisa Bonds, and Eva Ortiz-Smith. They were all helpful in one way or another. It was always a pleasure to work with or talk to them. I especially want to thank Marilyn Ownby for being such a delightful person. She is a wonderful asset to the chemistry department. To Emily Jones I owe a great deal of gratitude. She was a strong support to me during a time when I had issues with my health. She offered me great advice and became a dear friend to me. I will definitely miss her.

One of the greatest parts of being at the University of Tennessee was meeting so many people from so many different places. I was able to meet some great people and get to know them on a personal level, and I will always consider them my friends. Dr. Medhanit Bahta is very special to me. I remember the day she arrived in Knoxville from Eritrea, Africa. I consider her a part of my family. Brandy Belue was one of my dearest friends at UT. Although she has moved on, we still remain close. Eric Dadush became my lunch partner. I will miss our weekly trips for half-price hamburgers at the Cumberland Grill. Others who have been friends are members of Dr. Xue's group, including, Royce Dansby-Sparks, Dr. Li Yong, Dr. Jim Chen, Clarissa Tatum, Brenda Dougan, and Julia Covington Abbott. Royce and Li were important to my success, as they worked closely with

me on the electrochemistry experiments. They participated in many discussions on electrochemistry and bismuth electrodes.

I would also like to thank some people from my earlier studies. My undergraduate advisor, Dr. Charles Henry, inspired me to pursue research and encouraged me to go to graduate school. Without Dr. Henry, my life may have taken a different course. Also a great inspiration to me is my co-op supervisor, Sherry Scruggs. She taught me many analytical procedures and was a great role model for me. Mr. Bobby Worley, my high school chemistry teacher, gave me a foundation to build upon.

I owe the greatest appreciation to my family, who has been my constant support during my graduate studies. When I was hesitant to move out of my comfort zone to attend graduate school, they assured me that everything would be fine. My parents, Ritchie and Brenda Carter, have shown only love and support in all my endeavors. They have made me who I am now, and I love them with all my heart. My Mamaw, Donna Fox, became one of my closest friends, and I will always cherish our phone conversations. My brother, Sid, grew up while I was in Knoxville. I always enjoyed his visits during the summer. He was there for me during the loss of my dear Alley, and I would not have made it through that time without him.

To my husband Will, I thank him so much for being who he is and accepting who I am. He believed in me when I didn't believe in myself. I love him more than I can express through words.

ABSTRACT

An Advanced Oxidation Process (AOP) was designed for the decomposition of organic material in blood as a pretreatment for chromium analysis. Acidified porcine blood was treated with hydrogen peroxide and UV light for 60 min. The rate of decomposition was studied using UV/Vis spectroscopy. It was found that the order of the photolytic reaction with respect to hydrogen peroxide was 0.35. The pretreated blood was subsequently analyzed for chromium content by catalytic adsorptive stripping voltammetry at a bismuth film electrode. The concentration of chromium was determined to be 6.0 $\pm$ 0.3 parts per billion (ppb). A bismuth bulk electrode was designed and characterized, and was found to be useful in the analysis of Pb(II), Cd(II), and Zn(II) in environmental samples.

TABLE OF CONTENTS

LIST OF TABLES

LIST OF FIGURES

NOMENCLATURE AND ABBREVIATIONS

A	absorbance
AA	atomic Absorption
AOP	advanced oxidation process
ASV	anodic stripping voltammetry
BiBE	bismuth bulk electrode
BiFE	bismuth film electrode
°C	degrees Celcius
C	concentration
CAdSV	catalytic adsorptive stripping voltammetry
CV	cyclic voltammtery
DTPA	diethylene triamine pentaacetic acid
ε	molar absorptivity
g	gram
HMDE	hanging mercury drop electrode
k, *k'*, *k"*	rate or pseudo rate constants
L	liter
mM	millimolar
M	molar
MFE	mercury film electrode
mg	milligram

min	minute
mL	milliliter
nm	nanometer
ppm	parts per million
ppb	parts per billion
ppt	parts per trillion
R^2	square of correlation coefficient
rpm	rotations per minute
s	second
SWV	square wave voltammetry
t	time
TOC	total organic carbon
UV	ultraviolet radiation
UV/Vis	ultraviolet/visible spectrophotometry
W	watt
λ	wavelength

Part 1

Introduction and Background

1.1 INTRODUCTION

Diabetes is a common disease that affects 16 million people in the United States, with an estimated 800,000 new cases diagnosed each year.[1-4] Chromium is an essential trace element for mammals.[5-8] Chromium is found in many foods, such as some meats and fish, animal fats, coffee, tea, spices, whole-wheat and rye breads, and yeast. Cr complexes have been used as a dietary supplement for the treatment of diabetes and its complications.[1-4] Chromium deficiency has also been linked to increased risk of nonfatal myocardial infarction and cardiovascular disease.[9-11]

The frequency of actual chromium deficiency in the population is unknown in part because reliable measures for assessing chromium status in humans are limited.[12] Since the levels of chromium present in biological tissues and fluids are extremely low (e.g., ca. 3-10 ppb in blood of mammals)[13-19] and chromium is bound to peptides,[5-8] many difficulties associated with finding a measure of the chromium status are analytical in nature.[12] Currently there are three analytical techniques with the required sensitivity for the measurement of chromium in biological samples from humans:[12] neutron activation,[9-11] mass spectrometry [such as high resolution inductively coupled plasma mass spectrometry HR-ICP-MS or (dynamic reaction cell) DRC-ICP-MS],[12] and graphite furnace atomic absorption spectroscopy (GF-AAS).[20,21] The first two techniques require expensive instrumentation and are thus not widely available. In the chromium analysis by GF-AAS, the samples are usually heated to, e.g., 2500 °C for

pretreatment and atomization.[20,21] Heating to high temperature is needed in part to decompose biological/organic species and to release chromium from their complexes. This technique is highly susceptible to interference from the sample matrix.[12] In the ICP-MS and GF-AAS analysis of chromium in blood and tissue samples, a pretreatment step using microwave digestion is often needed.[13-15,17] There is an urgent need (1) to develop improved techniques for the analysis of chromium in biological fluids, and (2) to assess chromium deficiency and the effect of chromium as adjuvant therapy for Type 2 diabetes.

The research presented in this dissertation is a progression in the development of such a technique for the determination of chromium in biological samples and is encompassed by two parts: (1) the pretreatment of the biological sample to remove organic ligands and free chromium for analysis, and (2) the subsequent analysis of chromium (VI) at trace levels. The first step was to develop an Advanced Oxidation Process for the pretreatment of blood samples. When that part was achieved, a way to detect the chromium species was needed. Electrochemistry, more specifically, catalytic adsorptive stripping voltammetry at a bismuth film electrode was the only practical method sensitive enough for the task. After it was found that the bismuth film electrode was difficult to make and results were irreproducible, the research branched out into a different avenue of electrochemistry. With the development of the bismuth bulk electrode, it was possible to probe even further into the fundamental studies of the electrochemical detection of Cr(VI).

This has certainly been a diverse study, one that proves the interdisciplinary nature of chemistry. The projects involve biological chemistry, photochemistry, analytical chemistry, electrochemistry, and inorganic chemistry, as well as electrical engineering and kinetics.

1.2. TECHNIQUES USED IN THE RESEARCH

1.2.1. Advanced Oxidation Process

Advanced Oxidation Processes (AOPs) have been studied for the degradation of pollutants in wastewater and drinking water for over 30 years.[22-24] Traditionally, the treatment of wastewater involved the use of strong oxidants, such as chlorine, ozone, chlorine dioxide, and potassium permanganate. Oxidation destroys organic compounds by converting them into carbon dioxide, water, and inorganic ions. The use of ultraviolet (UV) irradiation enhances the oxidation process and the overall reaction rates. AOP is an oxidation process that specifically depends on the generation of reactive hydroxyl free radicals (•OH) as the oxidant initiating oxidative degredation.[22,25] The •OH radicals can be generated by both photochemical and nonphotochemical processes.[23] Next to fluorine, •OH radicals are the most potent oxidant with a standard reduction potential of 2.80 V. Table 1.1 lists the most common oxidants and their standard reduction potentials.

AOP is divided into four main groups: (1) vacuum ultraviolet (VUV) photolysis, (2) sensitized AOP processes, (3) ultraviolet (UV)/oxidation

Table 1.1. Standard reduction potentials of common oxidant species.[22]

Species	Standard Reduction Potential (V)
Fluorine	3.03
Hydroxyl Radical	2.80
Ozone	2.07
Hydrogen Peroxide	1.78
Permanganate	1.68
Chlorine	1.36

processes, (4) photo-Fenton processes.[23] VUV is the generation of •OH and H• radicals with UV irradiation at wavelengths below 190 nm. Sensitized AOP processes include the use of organic dyes or semiconductors. These two processes are not used in the current research and therefore will not be discussed. UV/H_2O_2 and photo-Fenton are discussed in detail below.

1.2.1.1. *UV/H_2O_2 Process*

As stated above, the key requirement for AOP is the production of •OH radicals, which become the oxidant in the decomposition of organic compounds. The most basic generation of •OH radicals is through the photolytic cleavage of H_2O_2 (Equation 1.1).[22-26]

$$H_2O_2 + h\nu \rightarrow 2\ \bullet OH \qquad \text{Equation 1.1}$$

The •OH radicals are a highly reactive transient that rapidly oxidizes organic substances.[27] There are three types of mechanisms for the reactions that take place between organic molecules and •OH.[24] They are

1) Hydrogen abstraction[24,28]

$$HO\bullet + RH \rightarrow R\bullet + H_2O \qquad \text{Equation 1.2}$$

2) Electrophilic addition

$$HO\bullet + RX \rightarrow HORX\bullet \qquad \text{Equation 1.3}$$

3) Electron transfer

$$HO\bullet + RX \rightarrow RX\bullet^{+} + HO^{-} \qquad \text{Equation 1.4}$$

Also generated in the process are other reactive species, such as hydroperoxyl or peroxyl radicals which, in turn, also help decompose organic compounds.

1.2.1.2. *Photo-Fenton Process*

The Fenton process, a dark process involving no UV irradiation, is the decomposition of H_2O_2 to •OH using the ferrous ion (Fe^{2+}) or ferric ion (Fe^{3+}) under acidic conditions. The main reactions that take place in the Fenton reaction are listed below:[28,29]

$$Fe^{2+} + H_2O_2 \rightarrow Fe^{3+} + \bullet OH + OH^{-} \qquad \text{Equation 1.5}$$

$$Fe^{3+} + H_2O_2 \rightarrow Fe^{2+} + HO_2\bullet + H^{+} \qquad \text{Equation 1.6}$$

$$Fe^{2+} + \bullet OH \rightarrow OH^{-} + Fe^{3+} \qquad \text{Equation 1.7}$$

$$H_2O_2 + \bullet OH \rightarrow HO_2\bullet + H_2O \qquad \text{Equation 1.8}$$

$$Fe^{2+} + HO_2\bullet + H^{+} \rightarrow Fe^{3+} + H_2O_2 \qquad \text{Equation 1.9}$$

$$Fe^{3+} + HO_2\bullet \rightarrow Fe^{2+} + O_2 + H^{+} \qquad \text{Equation 1.10}$$

As shown in these equations, iron is a catalyst in the process. The rate of decomposition and generation of •OH radicals are greatly increased by irradiation with UV light (Equation 1.11).

$$Fe^{3+} + H_2O + h\nu \rightarrow Fe^{2+} + H^+ + \bullet OH \qquad \text{Equation 1.11}$$

When Equations 1.5 and 1.11 are combined, the iron becomes cycled between +2 and +3 oxidation states, and two moles of •OH are produced per mole of H_2O_2 consumed.[22] The photo-Fenton reaction is the predominant process in the AOP of blood due to the large amount of biological iron present. Also, the reaction rate of the photo-Fenton process is fastest at pH 3.0.[22,28]

1.2.2. UV/Visible Spectrophotometry

When a molecule absorbs energy, specifically UV or visible radiation, an electronic transition occurs in which outer electrons are excited from their ground state to an excited state. The absorbance is measured by a UV/Vis spectrophotometer. The concentration of the absorbing species is directly related to the absorbance according to Beer's Law (Equation 1.12)[30]

$$A = \varepsilon b c \qquad \text{Equation 1.12}$$

where A is the absorbance, ε is the molar absorptivity ($M^{-1}cm^{-1}$), b is the pathlength (cm), and c is the concentration (M) of the analyte. UV/Vis

spectrophotometry was used in the study of AOP kinetics to monitor the decomposition of biological/organic components in blood as a function of time.

1.2.3. Electrochemical Techniques

Three electrochemical techniques were used in this research, cyclic voltammetry (CV), square-wave voltammetry (SWV), and anodic stripping voltammetry (ASV). In CV, a sweeping potential is applied to the system in both the forward and reverse directions, and the resulting faradaic current from the redox reaction is measured.[31] CV was used for the fundamental and surface studies of the BiBE, as well as the Cr-DTPA mechanism.

SWV is a pulse technique in which the potential is modulated to increase sensitivity. The waveform is basically a square wave superimposed onto a staircase waveform. The current is sample twice in each pulse, once in the forward half cycle and once in the reverse (Figure 1.1).[32] The generated signal is the difference between the two currents (Figure 1.2).[33] This technique has excellent sensitivity due to the fundamental elimination of background current.[31]

Anodic stripping voltammetry (ASV) is a sensitive method for the detection and quantitation of metals. ASV is especially advantageous because multiple metals can be detected simultaneously. In this technique, the metals are accumulated onto the electrode surface by applying a negative potential. A pulsed technique, such as SWV, is then used to sweep the potential in a positive direction to oxidize the plated metals. A current peak occurs corresponding to

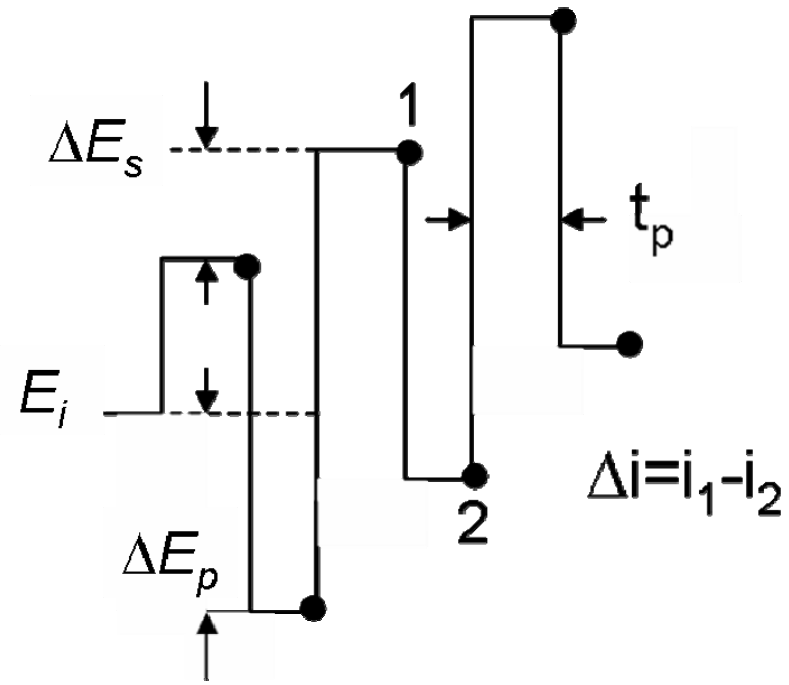

Figure 1.1. Common waveform for square wave voltammetry.[32] ΔE_s is the step height (the potential increment from one cycle to the next), ΔE_p is the pulse amplitude, and t_p is the pulse width. Heavy dots indicate the time at which current is sampled.

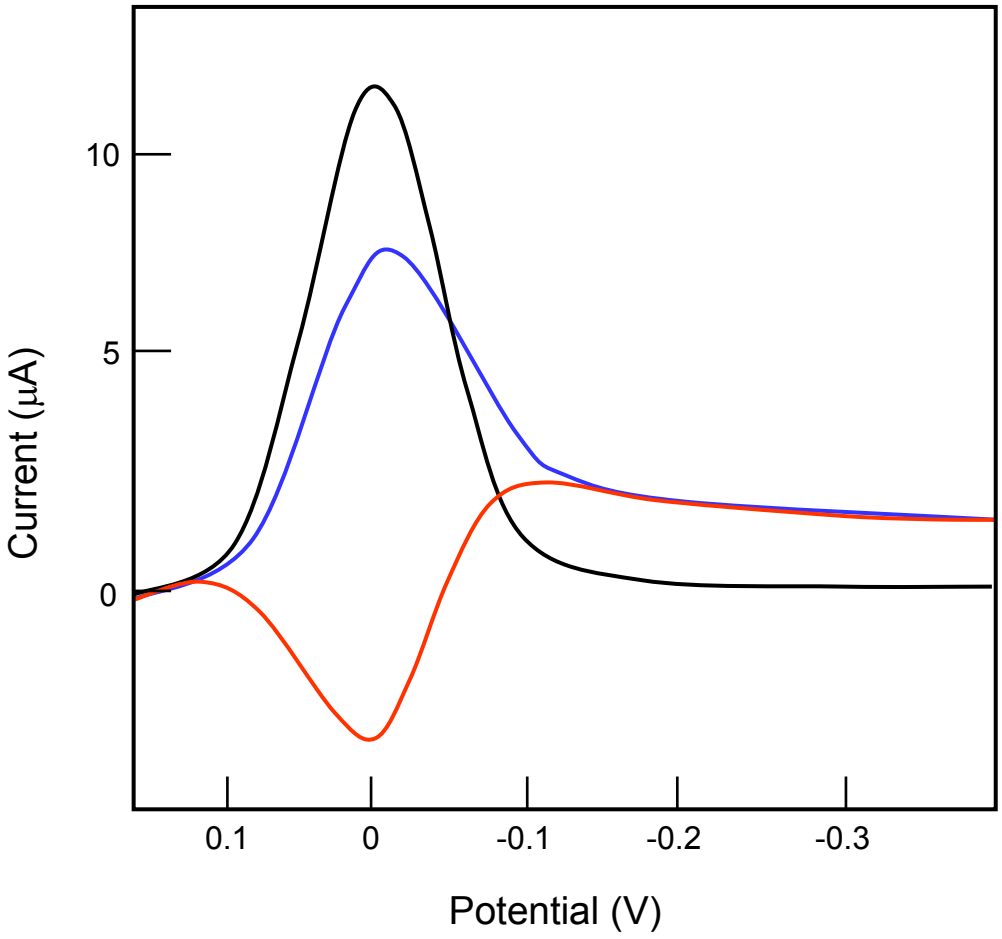

Figure 1.2. Voltammagrams corresponding to SWV; forward (blue), reverse (red), and net current (black).[33]

the oxidation, or stripping, of the individual metal from the electrode. The peak height is proportional to the metal concentration.

1.2.4. Bismuth Electrodes

Bismuth was recently introduced as a propitious material for electrode modification. Wang *et al.* report that a film of bismuth deposited onto a glassy carbon electrode exhibits the desirable electrochemical properties of mercury, yet it is non-toxic and environmentally friendly.[34] While Bi is not electrochemically inert due to the formation of bismuth oxide films and the subsequent dissolution of Bi(III) species, it does have a large overpotential for the evolution of hydrogen and a correspondingly large negative potential window, ranging from approximately -0.1 to -1.7 V (depending on pH).[35] Bismuth films electrodes (BiFE) have been studied extensively in the past seven years for the detection of many metal species. The detection of trace Cr(VI) by catalytic adsorptive stripping voltammetry (CAdSV) at the BiFE was reported by Lin *et al.* with detection limits in the low ppt range.[36] This technique was attractive for the analysis of Cr(VI) in AOP pretreated blood samples. However, during the course of this research, it was noted that the BiFEs were very difficult to prepare and calibration plots were unpredictable. Because of this, an electrode made of bulk bismuth (rather than a film) seemed like a robust alternative to the BiFE. At the time, there were two publications describing the designs and uses of BiBEs.[35,37] A BiBE was fabricated using a modified design of those reported.

1.3. SUMMARY OF DISSERTATION PARTS

1.3.1. Part Two

A new method for pretreating blood samples for trace Cr analysis is described in Part 2. The Advanced Oxidation Process (AOP with H_2O_2 and 5.5-W irradiation for 60 min) is used to remove biological/organic species for subsequent analysis. Prior to the AOP pretreatment, nitric acid is used to adjust the pH to 3.0 to inhibit the enzyme catalase in the blood samples. Catalytic Adsorptive Stripping Voltammetry (CAdSV) at a bismuth film electrode (BiFE) gives Cr concentration of 6.0 ± 0.3 ppb in the blood samples. This concentration was confirmed by dry-ashing the blood samples and subsequent analysis by atomic absorption spectroscopy (AAS). This current method may be used to monitor chromium, a trace metal in humans, and the efficacy and safety of chromium supplements as adjuvant therapy for diabetes.

1.3.2. Part Three

The study of the kinetics of the advanced oxidation process on blood is reported in Part 3. UV/Vis spectroscopy is used to monitor the change in absorbance with time in the AOP of blood. Most photochemical reactions are reported to follow zero-order kinetics. However, an extensive study of our AOP system proved to be more complex, perhaps due to the inherent Fenton and photo-Fenton processes, and showed non-zero order kinetic behavior. A new multi-cell reactor was designed to allow for multiple samples to be processed at

once. These kinetics were then compared to the single sample reactor to determine which design was more efficient. The distribution of UV irradiation to each sample was also evaluated.

1.3.3. Part Four

The design and characterization of a BiBE and its application for Cr(VI) detection is described in Part 4. The electrochemical mechanism of the Cr(VI) detection was studied at the BiBE by CV in order to gain an insight to the process. A similar study was done by Sander *et al.* at a hanging mercury drop electrode (HMDE).[38] The surface chemistry of the bismuth electrode proved to be comparable to that mercury. The BiBE proved not to be sensitive enough for trace Cr(VI) detection. Results from the mechanistic study of Cr detection at the BiBE and the lack of sensitivity for trace Cr(VI) detection are discussed in this section.

1.3.4. Part Five

Trace metal analysis of lead(II), zinc(II), and cadmium(II) with the BiBE by anodic stripping voltammetry is discussed in Part 5. Concentrations as low as 10 ppb were achieved using the novel electrode. Its linear dynamic range was from 10 ppb to 100 ppb. A sample from the Tennessee River was tested and the concentrations of the metals were found to be negligible. These experiments done with the BiBE are applicable for analyses of environmental samples.

REFERENCES

(1) Anderson, R. A. *J. Am. Coll. Nutr.* **1998**, *17*, 548-555.

(2) Anderson, R. A. *Nutr. Res. Rev.* **2003**, *16*, 267-275.

(3) Katz, S. A.; Salem, H. *The Biological and Environmental Chemistry of Chromium*; VCH: Weinheim, 1994.

(4) Ryan, G. J.; Wanko, N. S.; Redman, A. R.; Cook, C. B. *Ann. Pharmacother.* **2003**, *37*, 876-885.

(5) Dinakarpandian, D.; Morrissette, V.; Chaudhary, S.; Amini, K.; Bennett, B.; Van Horn, J. D. *BMC Chem. Bio.* **2004**, *4*, 2.

(6) Jacquamet, L.; Sun, Y. J.; Hatfield, J.; Gu, W. W.; Cramer, S. P.; Crowder, M. W.; Lorigan, G. A.; Vincent, J. B.; Latour, J. M. *J. Am. Chem. Soc.* **2003**, *125*, 774-780.

(7) Schwarz, K.; Mertz, W. *Arch. Physiol. Biochem.* **1959**, *85*, 292-295.

(8) Vincent, J. B. *Acc. Chem. Res.* **2000**, *33*, 503-510.

(9) Guallar, E.; Jimenez, F. J.; van 't Veer, P.; Bode, P.; Riemersma, R. A.; Gomez-Aracena, J.; Kark, J. D.; Arab, L.; Kok, F. J.; Martin-Moreno, J. M. *Am. J. Epidemiol.* **2005**, *162*, 157-164.

(10) Juturu, V.; Komorowski, J. R. In *Advances in Heart Failure (Proceedings of the World Congress on Heart Failure: Mechanisms and Management, 8th, Washington, DC)*; Medimont: Bologna, Italy, 2002, pp. 279-282.

(11) Rajpathak, S.; Rimm, E. B.; Li, T.; Morris, J. S.; Stampfer, M. J.; Willett, W. C.; Hu, F. B. *Diabetes Care* **2004**, *27*, 2211-2216.

(12) Veillon, C.; Patterson, K. Y. *J. Trace Elem. Exp. Med.* **1999**, *12*, 99-109.

(13) Bocca, B.; Alimonti, A.; Forte, G.; Petrucci, F.; Pirola, C.; Senofonte, O.; Violante, N. *Anal. Bioanal. Chem.* **2003**, *377*, 65-70.

(14) Granadillo, V. A.; Demachado, L. P.; Romero, R. A. *Anal. Chem.* **1994**, *66*, 3624-3631.

(15) Kunze, J.; Wimmer, M. A.; Reich, M.; Koelling, S.; Jacobs, J. J. *At. Spectrosc.* **2005**, *26*, 8-13.

(16) Morris, B. W.; Macneil, S.; Stanley, K.; Gray, T. A.; Fraser, R. *J. Endocrinol.* **1993**, *139*, 339-345.

(17) Rodushkin, I.; Odman, F.; Olofsson, R.; Axelsson, M. D. *J. Anal. At. Spectrom.* **2000**, *15*, 937-944.

(18) Veillon, C.; Lewis, S. A.; Patterson, K. Y.; Wolf, W. R.; Harnly, J. M.; Versieck, J.; Vanballenberghe, L.; Cornelis, R.; Ohaver, T. C. *Anal. Chem.* **1985**, *57*, 2106-2109.

(19) Veillon, C.; Patterson, K. Y.; Bryden, N. A. *Clin. Chem.* **1982**, *28*, 2309-2311.

(20) Kortenkamp, A. *NATO ASI Series, Series 2: Environment* **1997**, *26 (Cytotoxic, Mutagenic and Carcinogenic Potential of Heavy Metals Related to Human Environment)*, 35-53.

(21) Rukgauer, M.; Zeyfang, A. *Biol. Trace Elem. Res.* **2002**, *86*, 193-202.

(22) Parsons, S., Ed. *Advanced Oxidation Processes for Water and Wastewater Treatment*; IWA Publishing: London, 2004.

(23) *Handbook on Advanced Photochemical Oxidation Processes.* EPA, 1998.

(24) Legrini, O.; Oliveros, E.; Braun, A. M. *Chem. Rev.* **1993**, *93*, 671-698.

(25) Symons, J. M.; Worley, K. L. *J. Amer. Wat. Works Assn.* **1995**, *87*, 66-75.

(26) Schulte, P.; Bayer, A.; Kuhn, F.; Luy, T.; Volkmer, M. *Ozone Sci. Eng.* **1995**, *17*, 119-134.

(27) Zepp, R. G.; Faust, B. C.; Holgne, J. *Environ. Sci. Technol.* **1992**, *26*, 313-319.

(28) Sigman, M. E.; Buchanan III, A. C.; Smith, S. M. *J. Adv. Oxid. Technol.* **1997**, *2*, 415.

(29) De Laat, J.; Gallard, H. *Environ. Sci. Technol.* **1999**, *33*, 2726-2732.

(30) Skoog, D. A.; Holler, F. J.; Nieman, T. A. *Principles of Instrumental Analysis*, 5th ed.; Saunders College Pub.: Philadelphia, 1998.

(31) Kounaves, S. P. *Handbook of Instrumental Techniques for Analytical Chemistry*; Prentice Hall PTR: Upper Saddle River, NJ, 1997.

(32) Osteryoung, J. *Acc. Chem. Res.* **1993**, *26*, 77-83.

(33) O'Dea, J. J.; Osteryoung, J.; Osteryoung, R. A. *Anal. Chem.* **1981**, *53*, 695-701.

(34) Wang, J.; Lu, J. M.; Hocevar, S. B.; Farias, P. A. M.; Ogorevc, B. *Anal. Chem.* **2000**, *72*, 3218-3222.

(35) Pauliukaite, R.; Hocevar, S. B.; Ogorevc, B.; Wang, J. *Electroanal.* **2004**, *16*, 719-723.

(36) Lin, L.; Lawrence, N. S.; Thongngamdee, S.; Wang, J.; Lin, Y. H. *Talanta* **2005**, *65*, 144-148.

(37) Buckova, M.; Grundler, P.; Flechsig, G.-U. *Electroanal.* **2005**, *17*, 440-444.

(38) Sander, S.; Navratil, T.; Novotny, L. *Electroanal.* **2003**, *15*, 1513-1521.

Part 2

Pretreatment of Blood Samples by the Advanced Oxidation Process for Quantitative Analysis of Chromium

2.1. INTRODUCTION

A new process to pretreat blood samples for chromium analysis has been developed. This new process combines the AOP treatment (aqueous 0.2% H_2O_2 and a 5.5-W UV irradiation) with acid deactivation of the enzyme catalase in blood. This procedure leads to the successful decomposition of biological/organic species in blood, and the conversion of chromium in different oxidation states to chromate. Subsequent Cr analysis by Catalytic Adsorptive Stripping Voltammetry (CAdSV) at a bismuth film electrode (BiFE), which was recently developed by Wang and coworkers,[1] yields Cr concentration of 6.0 ± 0.3 ppb in the blood samples. This Cr concentration is consistent with that (6.19 ± 0.03 ppb for the same blood samples) determined by a combination of dry-ashing[2] and atomic absorption spectroscopy. The work is a rare, successful AOP treatment of blood samples.[3,4] The results are discussed here.

2.2. EXPERIMENTAL

2.2.1. Reagents

Potassium hydroxide (Certified ACS, Fisher), potassium nitrate (Certified ACS, Fisher), potassium oxalate (Certified ACS, Fisher), acetic acid (glacial, Fisher), nitric acid (70%, Trace Metal Grade, Fisher), sodium acetate (anhydrous, Certified ACS, Fisher), and diethylenetriaminepentaacetic acid (DTPA, ≥99%, Fluka) were used as received. H_2O_2 (3%) was freshly prepared from 30% H_2O_2

(Optima Grade, Fisher) and deionized water. Bi and Cr(VI) AA standard solutions (1000 mg/L, Aldrich) were diluted prior to use. The electrolyte solution contained 0.1 M sodium acetate and 0.25 M KNO_3, and its pH was adjusted to 6.0 with CH_3COOH. The DTPA solution (0.1 M) was prepared by dissolving the DTPA in water while slowly adjusting the pH to 6.0 with 25% NH_4OH (Fisher Scientific). Cr(VI) standards were prepared by diluting the appropriate amount of stock solution in electrolytes. Porcine blood samples were obtained from Wampler's Farm (Lenoir City, Tennessee). The blood was collected in 1-L bottles each containing 2 g of potassium oxalate to prevent coagulation.[5]

2.2.2. Photochemical Reactor and UV Lamps

Pretreatment of blood samples by AOP was carried out in a 20-mL photochemical reactor shown in Figure 2.1. The photoreactor consisted of an outer vessel containing the sample, water-jacketed quartz immersion well, and a UV lamp. The reactor was designed and built in house, except for the quartz immersion well, which was purchased from Ace Glass. The UV lamp was a 5.5-W quartz low-pressure cold cathode mercury gaseous discharge lamp (Ace Glass 12132-08).

2.2.3. Instrumentation

CAdSV experiments were conducted using Electrochemical Workstation 650A (CH Instruments, Austin, TX). The cell assembly consisted of a Bi-coated glassy carbon working electrode (3 mm diameter, Cypress Systems, 66-EE047),

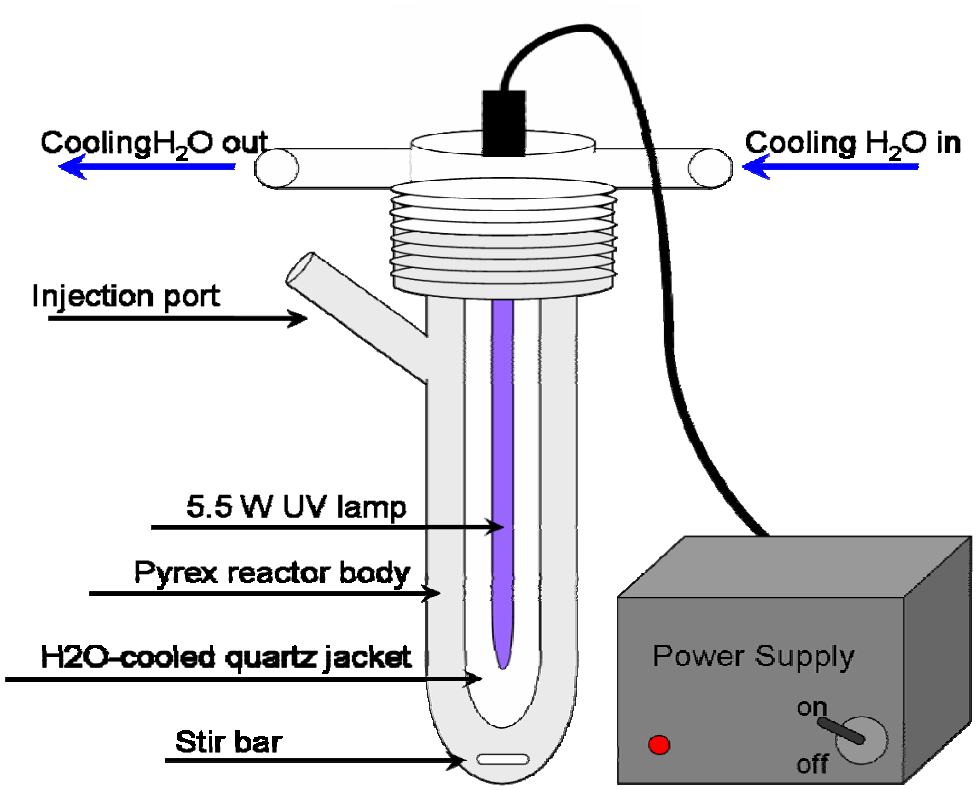

Figure 2.1. Schematic of photochemical reactor used in AOP experiments.

Ag/AgCl reference electrode (Model CHI111, CH Instruments), and a platinum wire counter electrode. The Bi coating was prepared by a procedure similar to that developed by Wang and coworkers.[1] A glassy carbon electrode was polished, exposed to piranha solution (1 part 30% H_2O_2 to 3 parts concentrated H_2SO_4), and sonicated prior to Bi coating. A 1.245 mg L^{-1} bismuth-0.1 M acetate buffer (pH 4.5) was prepared from a bismuth AA standard solution (1,000 ppm, Aldrich). The Bi coating onto the glassy carbon electrode was conducted at -1.20 V for 120 s. pH measurements were carried out with a pH meter (Accumet Basic, Fisher Scientific). All glassware was soaked in 1 M nitric acid and rinsed several times with deionized water prior to use. After a BiFE was prepared, standard solutions of Cr(VI) were analyzed by CAdSV. The standards ranged from 52 to 1311 ppt Cr(VI). The solution was first deaerated with nitrogen gas for 5 min. A DTPA solution was then added to a final concentration of 5 mM. Adsorption was carried out by holding the voltage at -0.8 V for 140 s while stirring. Square wave voltammetry (SWV) was performed in an unstirred solution over a potential range of -0.8 to -1.4 V with a potential step of 4 mV, an amplitude of 25 mV, a frequency of 20 Hz, and a quiet time of 8 s. The electrode was cleaned between each measurement by applying -1.2 V potential for 30 sec in the electrolyte solution. The SWVs were baseline corrected by subtraction of the background signal.

2.3. RESULTS AND DISCUSSION

2.3.1. An Advanced Oxidation Process

2.3.1.1. Inhibition of Catalase

When H_2O_2 was added to a diluted blood sample, vigorous foaming due to the decomposition of H_2O_2 by the enzyme catalase was observed. Although this enzyme protects the body from hydroxyl radicals,[6] the process to decompose H_2O_2 is detrimental to the AOP treatment of blood samples. To inhibit catalase activity, several reagents such as copper(II) sulfate, sodium cyanide, sodium azide, nitric acid, sodium-*n*-dodecyl sulphate (SDS), and 3-aminotriazole (ATA) have been used in the literature.[7,8] In choosing an optimal inhibitor for the deactivation of blood samples in the current work, we considered the following factors: (1) toxicity of the reagents – both NaCN and NaN_3 are extremely toxic; (2) the use of organic inhibitors such as SDS and 3-aminotriazole (ATA) requires their subsequent decomposition in the AOP step; (3) introduction of metal ions (in the use of $CuSO_4$) to the blood samples that may potentially contaminate the samples; (4) the use of KNO_3 in subsequent electrochemical detection of Cr(VI) by CAdSV.[1]

The structure of catalase is similar to that of cytochrome *c*, a protein responsible for electron transfer in the inner membrane of the mitochondrion. Both contain porphyrin heme groups. Literature reports the deactivation of cytochrome *c* at pH 3. Techniques such as circular dichroism, virbational

spectroscopy, and fluorescence spectroscopy have been used to establish conformational changes in cytochrome *c* at pH 3.[9] Due to the similarity in their structures, we believe catalase, at pH 3, undergoes a reorientation which renders it inactive.

We thus chose HNO_3 as the catalase inhibitor in the current work. Our tests revealed that the optimal pH for catalase inhibition was 3.0. To decompose the catalase and prevent the foaming, a 40 min irradiation of the sample under this acidic condition was essential.

2.3.1.2. Length of UV Irradiation

Earlier work conducted in our lab on the AOP pretreatment of chromium(III) propionate, a biomimetic chromium species, revealed that the optimal pH for 100% conversion of Cr(III) to Cr(VI) by AOP was 9.5.[10,11] Therefore, after the initial 40 min irradiation under acidic condition, a second AOP treatment of the blood sample at pH 9.5 for 20 min was used. Direct AOP treatment of blood sample under basic condition, or elimination of the first 40 min irradiation under acidic condition, was found to lead to vigorous foaming. Thus, AOP treatment at low pH followed by subsequent treatment at high pH was found necessary for complete and reproducible Cr(III) to Cr(VI) conversion.

2.3.1.3. Optimal H_2O_2 Concentration

The effect of AOP on the blood sample was visibly evident. When the blood sample was treated with 1.5 g/L H_2O_2, the bright red mixture turned to a

Figure 2.2. Blood samples before (left) and after (right) AOP with H_2O_2.

clear, faint yellow solution. The pretreatment method using 15 g/L H_2O_2 in an otherwise identical process turned the blood sample from a bright red mixture to a clear, nearly colorless solution with no observable precipitation (Figure 2.2). As discussed below, using 1.5 g/L H_2O_2 in the AOP treatment leads to more accurate Cr analyses by the CAdSV process.

2.3.2. Quantitative Analysis of Cr(VI) by Catalytic Adsorptive Stripping Voltammetry

2.3.2.1. *Catalytic Adsorptive Stripping Voltammetry*

CAdSV has shown very good sensitivity and low detection limits in the determination of ultratrace concentration of metals.[12-14] The Adsorptive Stripping Voltammetry (AdSV) technique is based on the accumulation of the analyte metal on a suitable working electrode by potential-controlled adsorption and subsequent electrochemical oxidation or reduction of the preconcentrated species. Coupling the adsorptive accumulation with a catalytic action leads to a significant increase of the analytical signal and the sensitivity of detection. Wang and coworkers recently developed the detection of Cr(VI) using Bi film electrode (BiFE) and CAdSV with a detection limit of 15.6 ppt Cr(VI).[1] In this procedure, Cr(VI) is reduced to Cr(III) electrochemically on the BiFE, and Cr(III) then binds to DTPA to yield an electroactive species $[Cr^{III}(H_2O)HY]^{-}$ [15,16] which is adsorbed onto the BiFE surface. $[Cr^{III}(H_2O)HY]^{-}$ is further reduced to $[Cr^{II}H_2Y]^{-}$ electrochemically at -1.1 V. Nitrate in the electrolyte solution oxidizes the Cr(II)

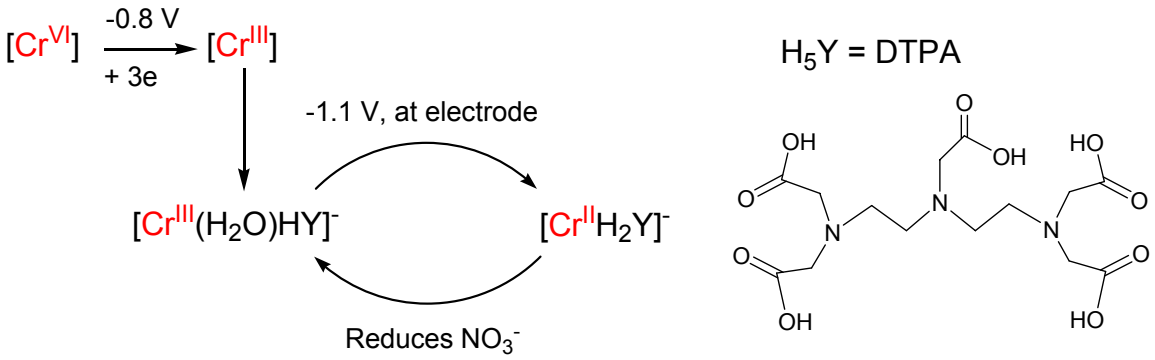

Figure 2.3. Mechanistic pathway in the detection of Cr(VI) species.[15,16]

species back to Cr(III) $[Cr^{III}(H_2O)HY]^-$ in a catalytic cycle, which significantly increases the SWV signal. Figure 2.3 demonstrates this cycle.[15,16]

With the mechanism of the CAdSV technique in mind, it is not difficult to understand the important role of electrolytes in precise CAdSV analyses. As shown in Figure 2.4, the effect of electrolytes in the CAdSV measurement of the AOP pretreated blood samples was quite clear. CAdSV was directly performed on an AOP pretreated blood sample (**Sample 1**) and a sample *after* the addition of electrolytes (KNO_3 and NaOAC to concentrations of 0.25 M and 0.1 M, respectively) and adjusting the pH to 6.0 (**Sample 2**). Without the electrolytes, the current peak for Cr in **Sample 1** is suppressed.

2.3.2.2. Effect of H_2O_2 on Blood Pretreatment by AOP and Measurement by CAdSV

One critical factor in AOP is the concentration of H_2O_2 during the UV irradiation. The role of H_2O_2 in AOP includes: (1) decomposition of organic ligands in blood samples, and (2) conversion of Cr at low oxidation states to Cr(VI) species. However, a high concentration of H_2O_2 is not desirable due to its negative influence in blood treatment and measurement. For blood pretreatment using AOP, a large concentration of hydroxyl radicals (•OH) increases the rate of their recombination, thus decreasing the AOP rate. Also, for measurements using CAdSV, a large excess of H_2O_2 in solution likely affects the catalytic cycle, as the mechanism in Scheme 1 suggests. The excessive H_2O_2 probably oxidizes the Cr(II) species back to Cr(III) $[Cr^{III}(H_2O)HY]^-$ and may affect the accuracy of

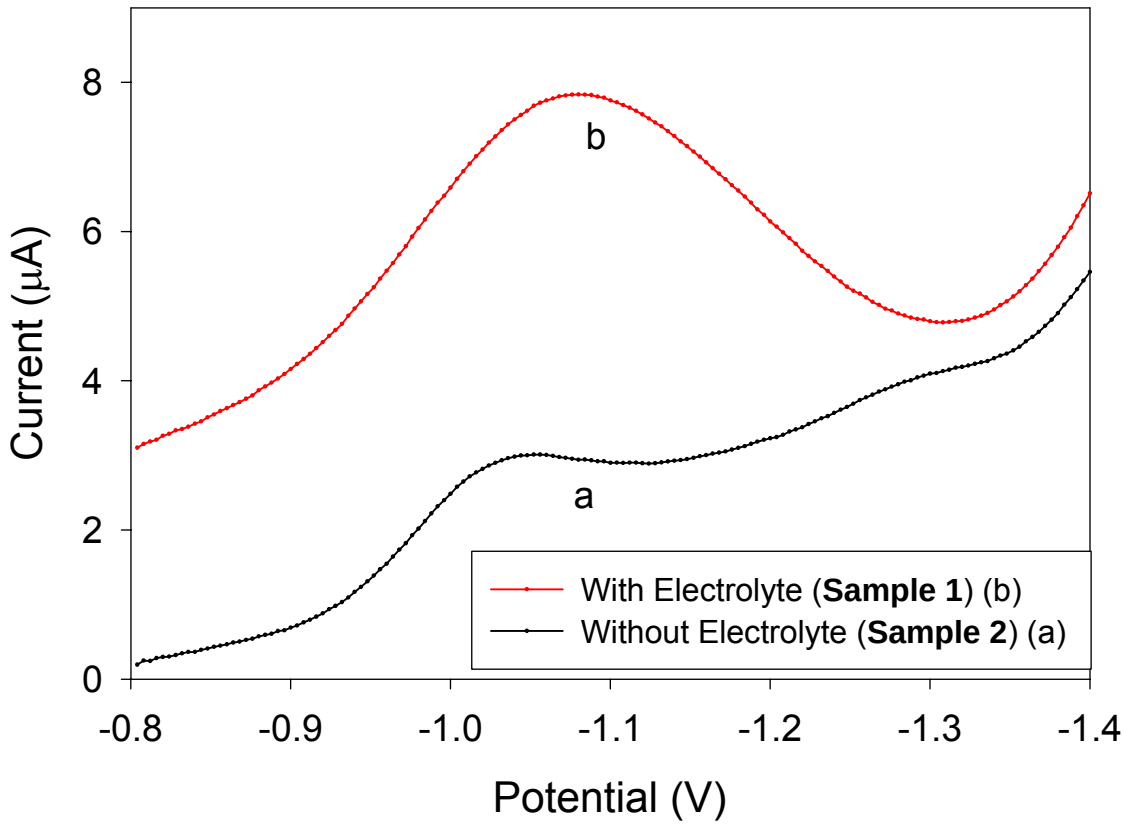

Figure 2.4. Square-wave voltammagrams of AOP-treated blood samples with and without electrolytes.

measurement. Thus, several experiments have been conducted to find the appropriate concentration of H_2O_2 that is both sufficient for AOP reaction and acceptable for measurement. Cr(VI) standard solutions (2.6 ppb) containing 0.0 g/L, 1.5 g/L, 3.0 g/L, and 8.3 g/L of H_2O_2 were analyzed by CAdSV. The influence of H_2O_2 at 1.5 g/L concentration level was found negligible (Table 2.1). In separate studies, AOP treatments of blood samples (0.5 mL diluted to 15 mL) were conducted with the H_2O_2 concentrations ranging from 0.75 g/L to 16.65 g/L. Each sample was UV-irradiated in the 20-mL photoreactor for 40 min. After careful screening, 2.0 g/L of H_2O_2 was found to be sufficient for the AOP treatment of the blood samples, and the concentration of H_2O_2 at up to 2.0 g/L does not interfere with the Cr(VI) measurement by CAdSV.

2.3.2.3. Calibration Plot and Measurement of Blood Samples

The SWVs and corresponding calibration plot for Cr(VI) standards measured by CAdSV at a BiFE in the current work are shown in Figures 2.5 and 2.6, respectively. The non-zero intercept on the calibration plot in Figure 2.6 is believed to be due to a Faradaic background current as a result of uncatalyzed reduction of nitrate in the absence of the Cr catalyst. With the standard calibration plot in hand, blood samples pretreated using AOP for 60 min (two UV irradiations) and a shorter 40 min (one UV irradiation) were analyzed by CAdSV. The blood samples treated by AOP for 60 min gave Cr concentrations of 6.0 $\pm$ 0.3 ppb. A dilution factor of 31 was used when calculating the Cr concentration. The Cr analysis of the sample after the shorter (40 min) AOP pretreatment

Table 2.1. The effect of H_2O_2 concentration on CAdSV analysis of standard 2.6 ppb Cr(VI) solutions (total volume: 20 mL).

Solutions	SWV current (μA)
Blank (buffer)	12.75
2.6 ppb Cr(VI)	20.38
2.6 ppb Cr(VI) + 1.5 g/L of H_2O_2	20.54
2.6 ppb Cr(VI) + 3.0 g/L of H_2O_2	31.99
2.6 ppb Cr(VI) + 8.3 g/L of H_2O_2	39.74

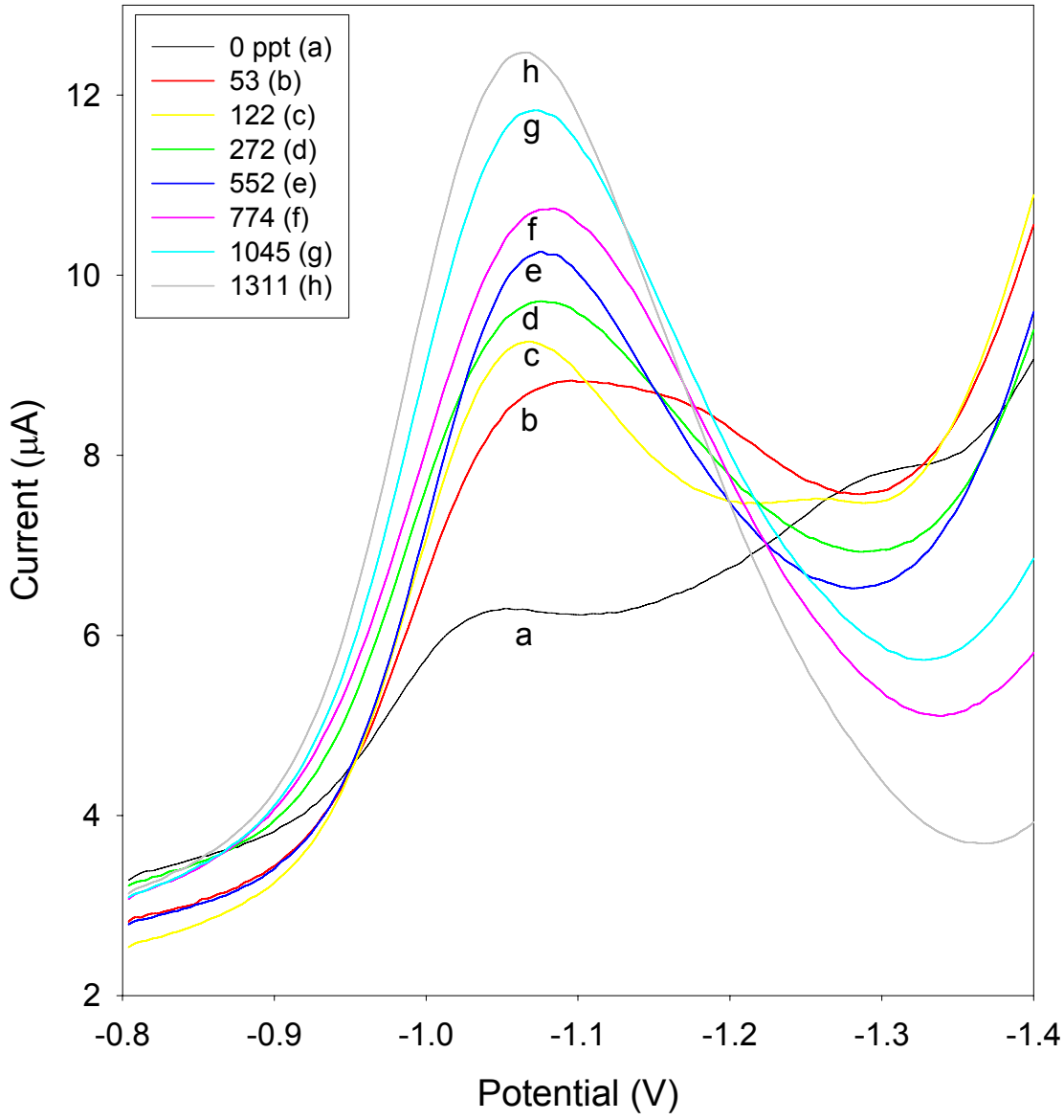

Figure 2.5. Square wave voltammagrams Cr(VI) standard solutions measured by CAdSV at a BiFE.

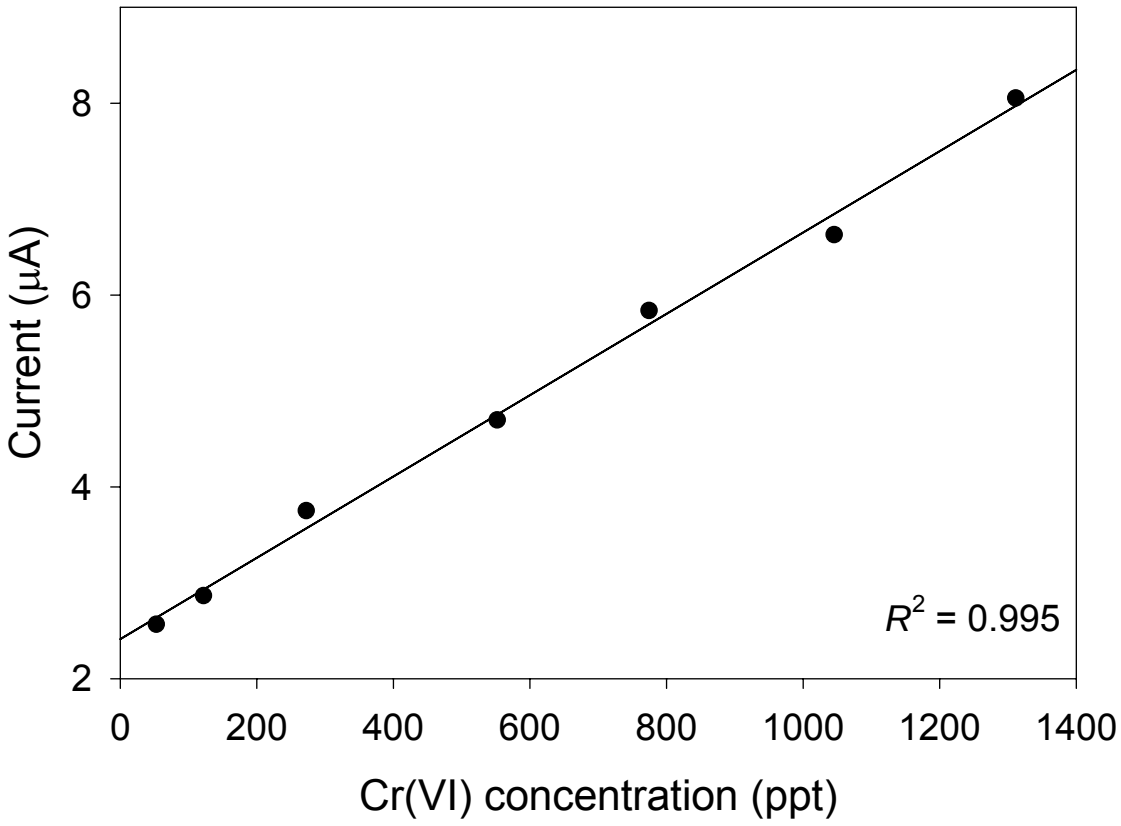

Figure 2.6. Calibration plot (bottom) of Cr(VI) standard solutions measured by CAdSV at a BiFE. The current of the blank was subtracted from those of samples in the calibration plot.

yielded 5.4 ± 0.3 ppb. As discussed below, dry-ashing followed by AA analysis as well as Cr spiking tests of the same blood sample gave Cr concentration of 6.19 ± 0.03 and 6.1 ± 0.2 ppb, respectively. In other words, the pretreatment using two UV irradiations, first at pH 3.0 for 40 min and then at pH 9.5 for 20 min, gives more accurate Cr(VI) concentration of the blood sample. This finding is in accord with our previous study on the AOP pretreatment of biomimetic chromium(III) propionate.[10,11]

Standard spiking is commonly used in analytical chemistry as a means of method validation. To test the accuracy and sensitivity of our technique, two blood samples were spiked with known amounts of Cr(VI): 260 ppt Cr(VI) and 780 ppt Cr(VI) in separate tests. CAdSV analysis of these two blood samples gave Cr(VI) concentrations of 414 ppt and 927 ppt, respectively (Figure 2.6). This gives Cr(VI) concentrations in the blood of 6.2 ppb and 5.9 ppb after the subtraction of the spiked standard. These concentrations correspond to the data obtained by direct analysis of the blood, and their average is 97% of the value from dry-ashing and AAS, which is discussed below.

2.3.2.4. Validation of Method by Dry-Ashing and Atomic Absorption Spectroscopy

Dry-ashing and subsequent Cr analysis by AAS of the blood samples were conducted to assess the accuracy of the Cr analysis by a combination of AOP with CAdSV developed in the current work. A sample from blood batch used in AOP and subsequent analysis by CAdSV was dry-ashed by heating a

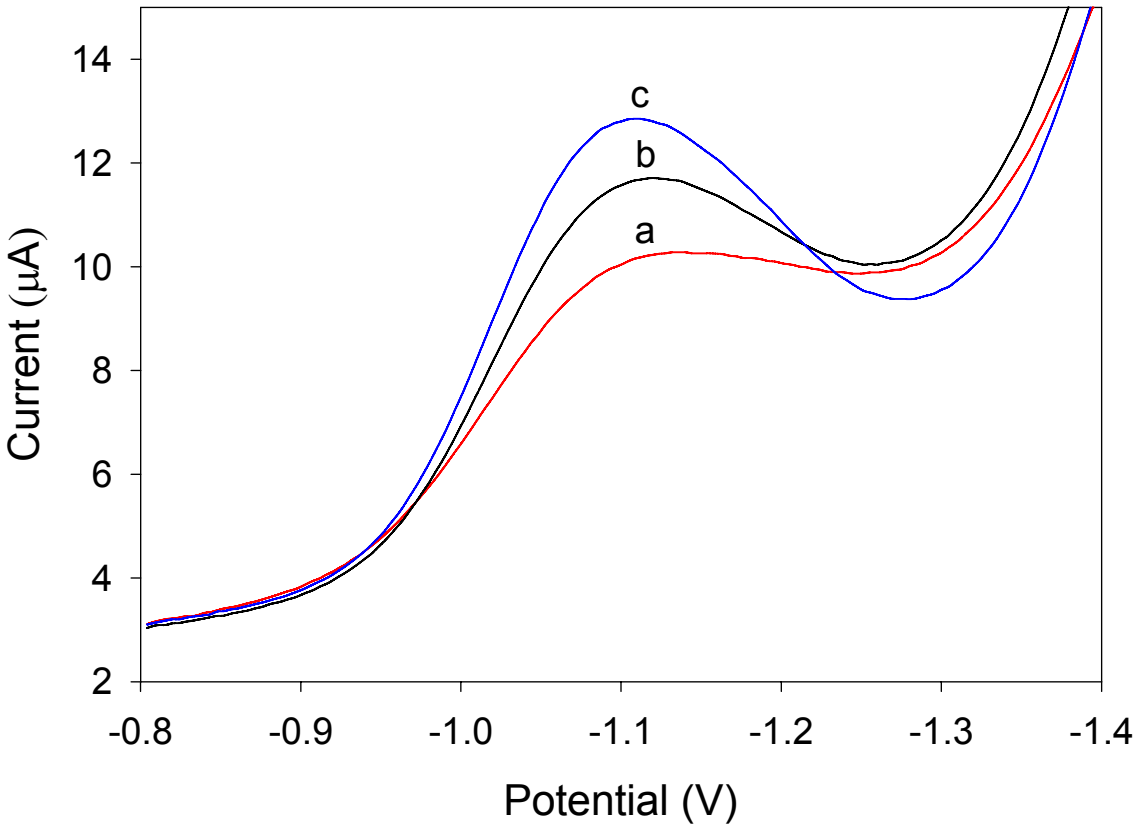

Figure 2.7. SWVs of AOP pretreated blood samples spiked with 0 ppt (a), 260 ppt (b), and 780 ppt (c) Cr(VI).

100-mL (100.0303 g) sample slowly and gently on a flame in a large evaporating dish to remove water. After the volume of the sample was decreased by 50%, the temperature of the flame was increased and the sample was heated for 3 h.

The sample was then carefully transferred to a quartz crucible and heated for another 2 h until only a small amount of inorganic residue remained. The weight of the final residue with a brick-red color was 0.9386 g. This residue was then dissolved in 10 mL of concentrated HNO_3. The solution was heated at 70 °C until all solid was dissolved. The solution was heated to concentrate the volume to 1 mL. Atomic absorption spectroscopy was then used for the measurement of the Cr concentration of the solution. The Cr concentration in the blood was found to be 6.19 ± 0.03 ppb.

2.3.2.5. *BiFE Reproducibility*

During the course of this study, it was found that the fabrication of the BiFE was difficult and the reproducibility was low. Even when the Bi film was successfully deposited onto the glassy carbon electrode, the resulting calibration plots of Cr(VI) standards were unsatisfactory. It seems the use of the BiFE is as much an art as it is a science.

2.4. Concluding Remarks

The current work shows chromium content at the ppb level in blood samples is easily analyzed through the use of the Advanced Oxidation Process (H_2O_2 and 5.5-W UV irradiation), followed by CAdSV using a BiFE.[17] The

concentration of 6.0 ± 0.3 ppb chromium in the AOP-treated sample is consistent with that determined by a combination of dry-ashing and AAS. AOP, after the chemical deactivation of the enzyme catalase, offers a fast, clean and inexpensive method for removing organic biological/organic species in blood.

REFERENCES

(1) Lin, L.; Lawrence, N. S.; Thongngamdee, S.; Wang, J.; Lin, Y. H. *Talanta* **2005**, *65*, 144-148.

(2) Bock, R. A. In *Handbook of Decomposition Methods in Analytical Chemistry*; Wiley: New York, 1979, Chapter 5.

(3) He, B.; Jiang, G. B.; Xu, X. B. *Fresenius J. Anal. Chem.* **2000**, *368*, 803-808.

(4) Pisch, J.; Schaefer, J.; Frahne, D. *GIT Fachz. Lab.* **1993**, *37*, 500-502, 504-505.

(5) Standard blood collection tubes, such as Vacutainer from Beckton, Dickinson, and Co. (www.BD.com), contain 2 mg/mL potassium oxalate (an anticoagulant) and 2.5 mg/mL sodium fluoride (a preservative). We modified this standard procedure to contain just the anticoagulant.

(6) Berg, J. M.; Tymoczko, J. L.; Stryer, L. In *Biochemistry,* 5th ed.; Freeman: New York, 2002, p. 506.

(7) Ghadermarzi, M.; Moosavi-Movahedi, A. A. *Biochim. Biophys. Acta* **1999**, *1431*, 30-36.

(8) Ito, O. *Nippon Jui Chikusan Daigaku Kiyo (Bull. Nippon Vet. Zootech. Coll.)* **1974**, *23*, 45-48.

(9) Cheng, Y. Y.; Lin, S. H.; Chang, H. C.; Su, M. C. *J. Phys. Chem. A* **2003**, *107*, 10687-10694.

(10) Rodman, D. L., Ph.D. Dissertation, The University of Tennessee, Knoxville, 2005.

(11) Rodman, D. L.; Carrington, N. A.; Xue, Z. L. *Talanta* **2006**, *70*, 668-675.

(12) Wang, J.; Lu, J. M.; Hocevar, S. B.; Farias, P. A. M.; Ogorevc, B. *Anal. Chem.* **2000**, *72*, 3218-3222.

(13) Yang, Y. J.; Huang, H. J. *Anal. Chem.* **2001**, *73*, 1377-1381.

(14) Zevin, M.; Reisfeld, R.; Oehme, I.; Wolfbeis, O. S. *Sens. Actuators* **1997**, *B38-39*, 235-238.

(15) Li, Y. J.; Xue, H. B. *Anal. Chim. Acta* **2001**, *448*, 121-134.

(16) Sander, S.; Navratil, T.; Novotny, L. *Electroanalysis* **2003**, *15*, 1513-1521.

(17) Yong, L.; Armstrong, K. C.; Dansby-Sparks, R. N.; Carrington, N. A.; Chambers, J. Q.; Xue, Z. *Anal. Chem.* **2006**, *78*, 7582-7587.

Part 3

Kinetic Studies of the Advanced Oxidation Process of Blood

3.1. INTRODUCTION

The kinetics of numerous organic-based AOP systems has been studied. Zero-order,[1] first-order,[2] pseudo-first order,[3-5] and second-order[6,7] kinetics have been reported on UV/H_2O_2, Fenton, and photo-Fenton processes. Sigman *et al*. found that both the •OH radical reaction with H_2O_2 and organic contaminants were pseudo-first order. However, they concluded that the overall rate of carbon loss was zero-order and varied as a function of chemical structure of the organic component.[1] The kinetics of the blood AOP system was studied, and the results are discussed below.

3.2. EXPERIMENTAL

3.2.1 Reagents

Porcine blood was collected in 1 liter plastic bottles containing 2 g of potassium oxalate (Fisher) diluted into 2 mL of H_2O. Upon collection, the blood was mixed well with the potassium oxalate to prevent coagulation. Concentrated nitric acid (Fisher) was used to adjust the pH of the blood. Hydrogen peroxide (30%, Fisher) was used for the AOP experiments. Deionized water (18 MΩ) was used in the preparation of aqueous solutions. Potassium hydroxide (Fisher) was used to adjust the pH of the blood in the second step of the AOP process. Titrations for the determination of H_2O_2 concentrations before and after AOP

treatment were done using potassium permanganate (Fisher) and concentrated sulfuric acid (Fisher).

3.2.2. Instrumentation

UV-Visible spectra were collected using a Hewett-Packard 8452 photodiode array spectrophotometer and a standard 1.0 cm quartz cuvette. Blank spectra of deionized water were recorded and subtracted from those of the samples.

3.2.3. Photochemical Reactors and UV Lamps

3.2.3.1. *Single-Sample AOP Reactor*

The reactor used in the AOP experiments consisted of a 20 mL cylindrical reactor vessel in which the sample was placed, a water-cooled quartz immersion well (Ace Glass), and a 5.5 W UV lamp and power supply (Pen-Ray). The reaction vessel was built in-house. A schematic representation of the AOP reactor is shown in Figure 2.1.

3.2.3.2. Multi-Sample AOP Reactor

A second AOP reactor was designed and built in-house. The idea of using the new reactor was two-fold: (1) process multiple samples at once, and (2) use a smaller volume of blood for each sample. The reactor is made of a base that contains four stirrers fashioned from small muffin fans purchased from a computer supply store. A magnet was attached to the top of each fan using

epoxy. The stirrers were placed in a custom-made box and controls were added. The top of the reactor box was designed to allow a water-cooled quartz immersion well (Ace Glass) to be inserted horizontally over the sample stirrers. A 100 W UV lamp (Hanovia) is then inserted into the immersion well. This set-up is then placed in a black box to contain any dangerous UV light. A power supply for the 100 W UV lamp is kept outside the box. A schematic of the multi-sample AOP reactor is shown in Figure 3.1. Cells for the reactor were made from square borosilicate tubing with dimensions insert dimensions here. The final volume for each was determined to be 5 mL.

3.2.4. Monitoring of AOP of Blood by UV/Vis Spectroscopy

The kinetics of the Advanced Oxidation Process on blood samples were studied using UV/Vis spectrophotometry. These experiments were conducted by following the concentration of the biological, UV- and visible-absorbing species in the blood, [blood]. According to Beer's law, the absorbance is directly proportional to the concentration of an analyte. In the current experiments of blood, there is not one particular analyte being monitored. The concentrations monitored in these kinetic experiments are thus designated as [blood].

3.2.4.1. *Experiments with the Single-Sample, 5.5 W AOP Reactor*

Kinetic experiments were conducted by measuring the UV/Vis absorbance of the AOP treated blood samples at different time intervals during the process. A 1-L batch of blood was prepared so that its composition would be the same for all

Figure 3.1. Photo of the multi-sample AOP reactor.

experiments. For this blood sample, 32.5 mL of blood was diluted with 975 mL of deionized H_2O in a large beaker. The pH was adjusted to 3.0 with concentrated HNO_3. It was transferred into a plastic 1 L bottle and stored in the refrigerator until use. For each individual AOP reaction, 15 mL of the diluted, pH-adjusted blood solution was transferred into the AOP reactor. An appropriate amount of 30% H_2O_2 was then added so that the final concentration was 1.5, 3.0, 5.0, 7.0, 8.0, 13.0, or 15.0 g/L H_2O_2. The immersion well was inserted and the stirring and UV lamp was turned on. After one minute of UV irradiation, UV irradiation was stopped and a small amount of the solution was pipetted into a 1 cm quartz cuvette. The UV/Vis spectrum was recorded. The AOP reactor was rinsed and dried thoroughly and a new aliquot of the prepared blood was added, as well as the specified amount of H_2O_2. The UV lamp was turned on. This time, the reaction was allowed to proceed for 2 min at which time the UV irradiation was stopped and a small sample was taken for UV/Vis analysis. This procedure was repeated for each minute for the first 10 min, and then every 5 min thereafter up to 40 min. After 40 min, the pH of the sample is adjusted to >9.0 by adding a few drops of KOH to the reactor. The UV was turned on again. A sample is taken for monitoring by UV/Vis after 5 min. The procedure is repeated until a total reaction time of 60 min.

3.2.4.2. *Experiments with the Multi-Sample AOP Reactor*

The preliminary experiments conducted with the multi-sample AOP reactor were designed to compare the efficiency of the 100 W UV lamp with multiple

samples to that of the 5.5 W lamp with a single sample. Also of interest was the UV irradiation distribution to each sample position of the multi- sample reaction. To aid with equal light distribution and act as a reflector, a piece of aluminum was placed above the UV lamp and along the side walls of the reactor.

The UV/Vis experiments were carried out as discussed previously, just with smaller volumes. The final of blood used in each reactor cell was 3 mL. Four samples were processed simultaneously. At given time intervals, the AOP was stopped and a sample from each cell was taken for UV/Vis analysis.

3.2.5. Determination of H_2O_2 Concentration before and after AOP

The determination of the concentration of H_2O_2 both before and after AOP was important in deciphering the kinetics of the process. The most commonly used titration method for the determination of H_2O_2 concentration is the permanganate method. It is accurate to 0.1 mg/L in both concentrated and dilute solutions.[8] The titration is based on the following reaction:

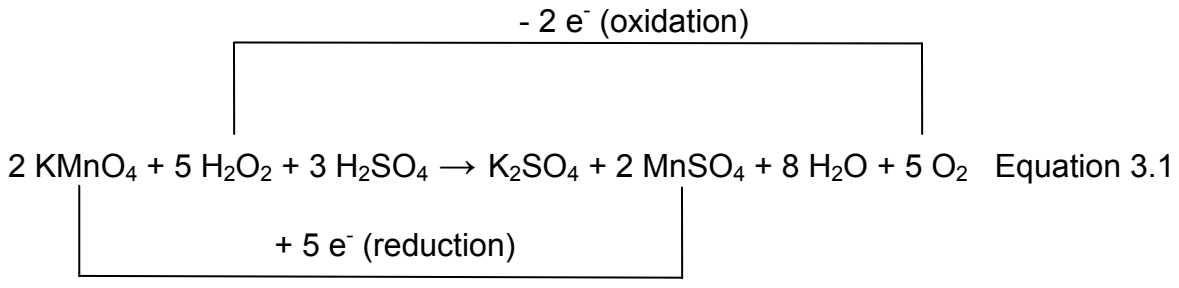

Equation 3.1

A $KMnO_4$ solution with a concentration of 0.1 M was prepared and standardized with potassium oxalate. The actual concentration was found to be

0.0949 M $KMnO_4$. After the completion of AOP, a sample of the blood was transferred into a 250 mL Erlenmeyer flask containing 100 mL of H_2O and 2 mL of concentrated H_2SO_4. The volume of the blood sample used for the titration depended on the concentration of the H_2O_2. For higher concentrations of H_2O_2, i.e., 15 and 8.3 g/L, 3 mL of the AOP sample were needed. For lower concentrations, i.e., 3.0 and 1.5 g/L H_2O_2, 5 mL of the sample were required. The solution was then heated on high heat for 3 min to a temperature of approximately 50 °C. Next, the solution was titrated with the standardized $KMnO_4$. During the titration, the purple MnO_4^- becomes nearly colorless as it is reduced to Mn(II) by H_2O_2. The endpoint is indicated by the return of the faint purple color. The volume of $KMnO_4$ used for the titration was recorded. The concentration of H_2O_2 was then calculated.

3.3. RESULTS AND DISCUSSION

3.3.1. An Advanced Oxidation Process for Blood

AOP has successfully been developed for the pretreatment for blood samples. It has been found that a combination the following processes contribute to the generation of •OH radicals and the overall efficiency of the method:[7,9-10]

1) Photolysis of H_2O_2

$$H_2O_2 + h\nu \rightarrow 2\ \bullet OH \qquad \text{Equation 1.1}$$

2) A Fenton process that produces hydroxyl radicals through the series of reactions in Equations 1.5–1.10

3) A photo-reduction of aqueous ferric ions in the Fenton process

$$Fe^{3+} + H_2O + h\nu \rightarrow Fe^{2+} + H^+ + \bullet OH \qquad \text{Equation 1.11}$$

The third step is probably the dominant mechanism of •OH production during later reaction times.[10] The AOP process was found to decompose the blood fastest when the highest concentration of H_2O_2 (15 g/L) was used.

3.3.2. Monitoring AOP of Blood by UV/Vis Spectroscopy

The decomposition of the organic components of blood during AOP was monitored by UV/Vis spectroscopy. Examples of the UV/Vis spectra obtained during AOP are given in Figures 3.2 and 3.3.

3.3.2.1. *Choice of Absorbance Wavelength*

The UV/Vis recorded spectra in the region of 200-800 nm. When processing the data, the absorbance values at 540 nm were used because of the presence of a peak in the diluted blood sample at pH 3 that decreased as a function of AOP time. It was later noticed that the UV portion of the spectra (200-300 nm) was maxed out. At this time, the experiments with 1.5 and 15 g/L H_2O_2 were performed again. Instead of using samples straight from the AOP reactor, samples were diluted in the UV/Vis quartz cuvette by using 250 μL of AOP blood

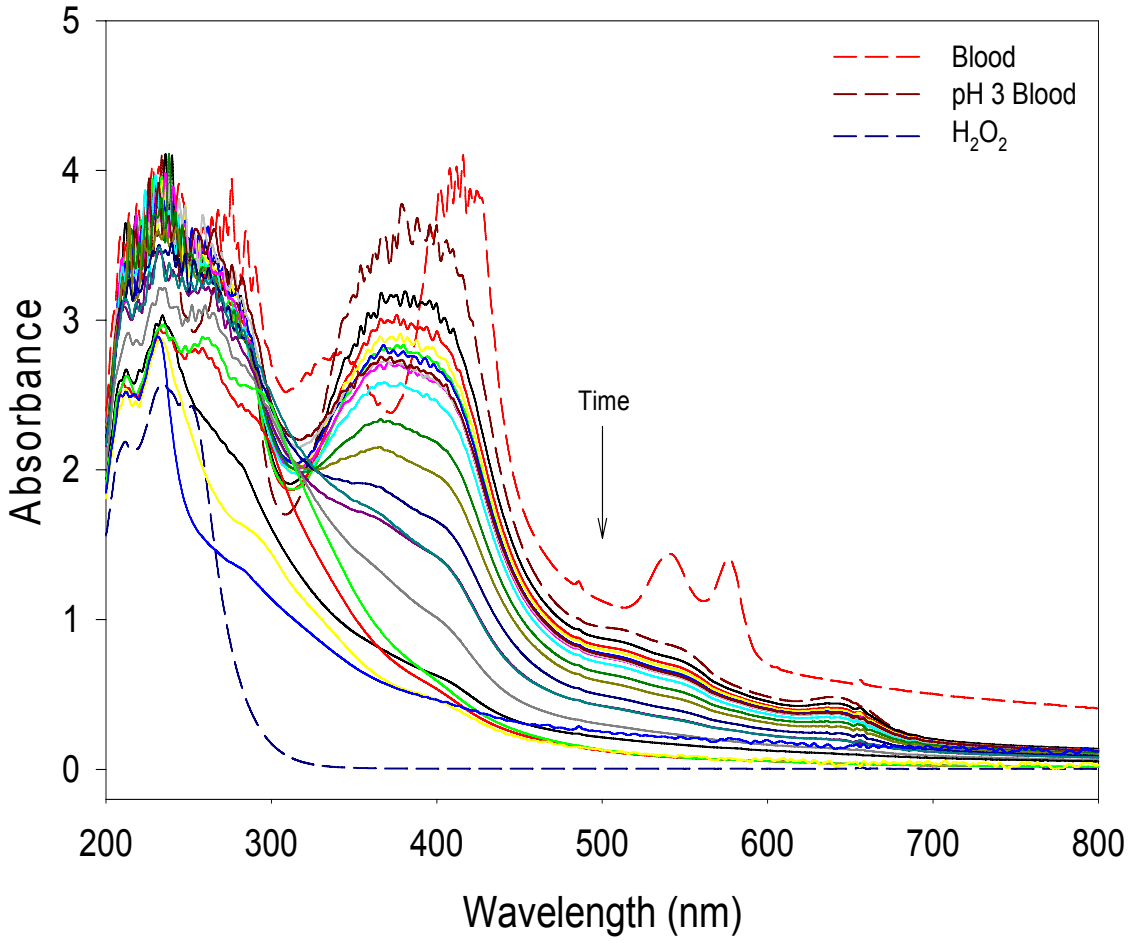

Figure 3.2. UV/Vis spectrum of blood AOP with 1.5 g/L H_2O_2. Spectra, taken every minute for the first 10 min and every 5 min for the last 30 min, show the decrease in absorbance during the AOP process.

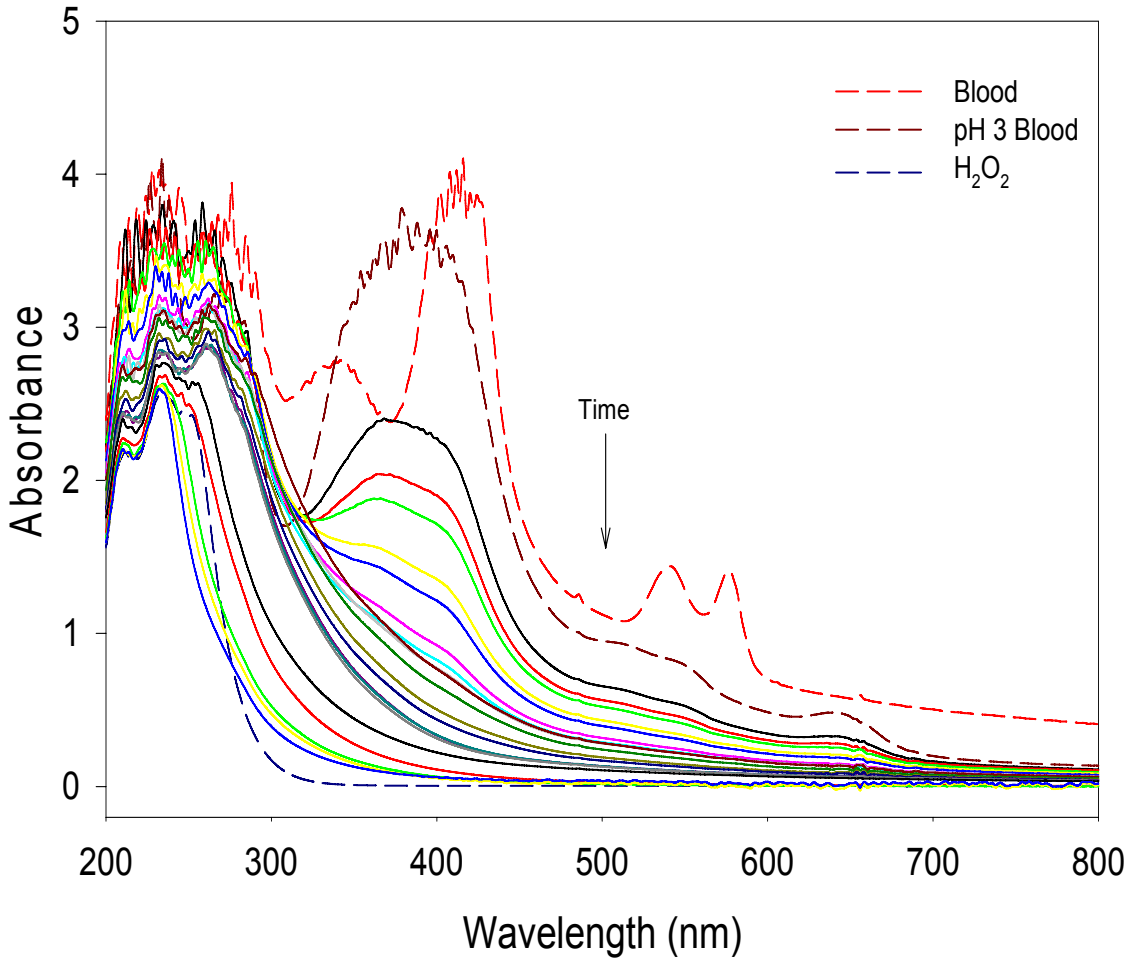

Figure 3.3. UV/Vis spectrum of blood AOP with 15 g/L H_2O_2. Spectra, taken every minute for the first 10 min and every 5 min for the last 30 min, show the decrease in absorbance during the AOP process.

and 2.75 mL of H_2O. This allowed for peaks previously undetected in the UV region to be observed. A peak at 540 nm in the visible spectra was chosen to follow during the kinetic experiments, again due to its decrease with AOP time. The new data was plotted with absorbance values at 540 nm versus time. These plots followed the same trend as that with the undiluted AOP samples. Therefore, not all of the experiments were re-evaluated. It should be pointed that H_2O_2 absorbs in the low UV range below 300 nm, with its maximum absorbance at 220 nm.[22]

3.3.2.2. *Effect of H_2O_2 Concentration*

As evident by both visually (Figure 3.4) and spectroscopically (Figure 3.5), a higher concentration of H_2O_2 results in a faster AOP time. H_2O_2 has a low molar extinction coefficient of 19.6 $M^{-1}s^{-1}$ at 254 nm, compared to 3300 and 10,000 $M^{-1}s^{-1}$ for ozone and pentachlorophenol, respectively.[11] Therefore a higher concentration of H_2O_2 is needed to produce a sufficient amount of •OH radicals. However, too high of a concentration of H_2O_2 tends to scavenge the •OH radicals, rendering the process less effective. The following equations demonstrate the scavenging effect:[11]

$$\bullet OH + H_2O_2 \rightarrow HO_2\bullet + H_2O \qquad \text{Equation 3.2}$$

$$HO_2\bullet + H_2O_2 \rightarrow \bullet OH + H_2O + O_2 \qquad \text{Equation 3.3}$$

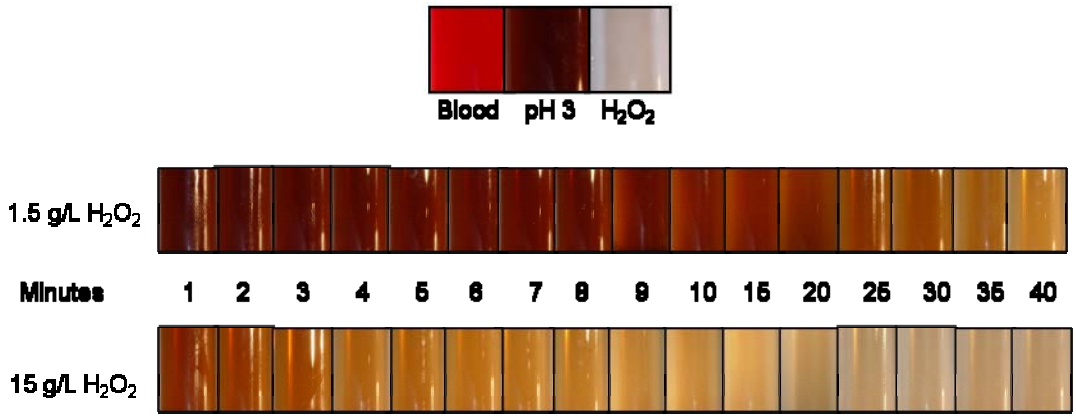

Figure 3.4. Visual representation of the change in color (or concentration of blood) with time during the AOP process with 1.5 and 15 g/L H_2O_2.

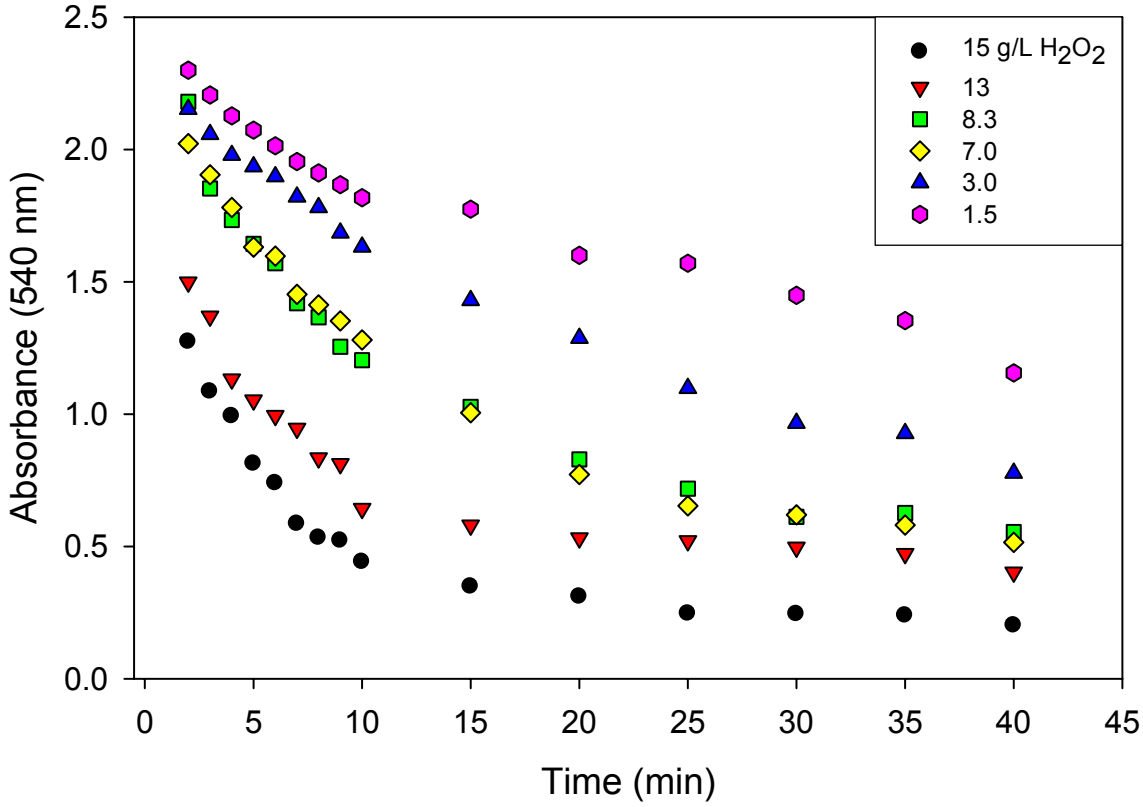

Figure 3.5. Monitoring AOP of blood by UV/Vis spectrophotometry with different concentrations of H_2O_2. The absorbance at 540 nm versus time is plotted.

$$HO_2\bullet + HO_2\bullet \rightarrow H_2O_2 + O_2 \qquad \text{Equation 3.4}$$

3.3.2.3. *Multi-Sample Reactor*

The absorbance of AOP blood samples from the multi-sample reactor was monitored by UV/Vis. The concentration of H_2O_2 was 15 g/L. Four samples were processed simultaneously in the home-made reactor with a 100-W UV lamp. The UV/Vis spectrum of each sample per unit of time was recorded. The absorbance at 500 nm was plotted versus time to compare to a 15 g/L H_2O_2 AOP blood sample processed in the single-sample reactor with a 5.5-W lamp. The result is shown in Figure 3.6. The plot shows a curve for each individual sample (circles) and a curve for the average of all four samples (diamond). The average indicates that the UV light is distributed differently to each sample, although the difference is small. When the plot is overlaid with the absorbance versus time plot for 15 g/L H_2O_2 AOP blood, the decomposition is almost identical. This indicates that the multi-sample reactor with a stronger lamp has the same efficiency, as far as time, as the single-sample reactor. Although the AOP time was not shortened with this reactor, its advantages are smaller sample volumes and the ability to run multiple samples simultaneously. A more efficient design should be considered in the future, perhaps one where the lamp is centered inside of a circle of multiple samples.

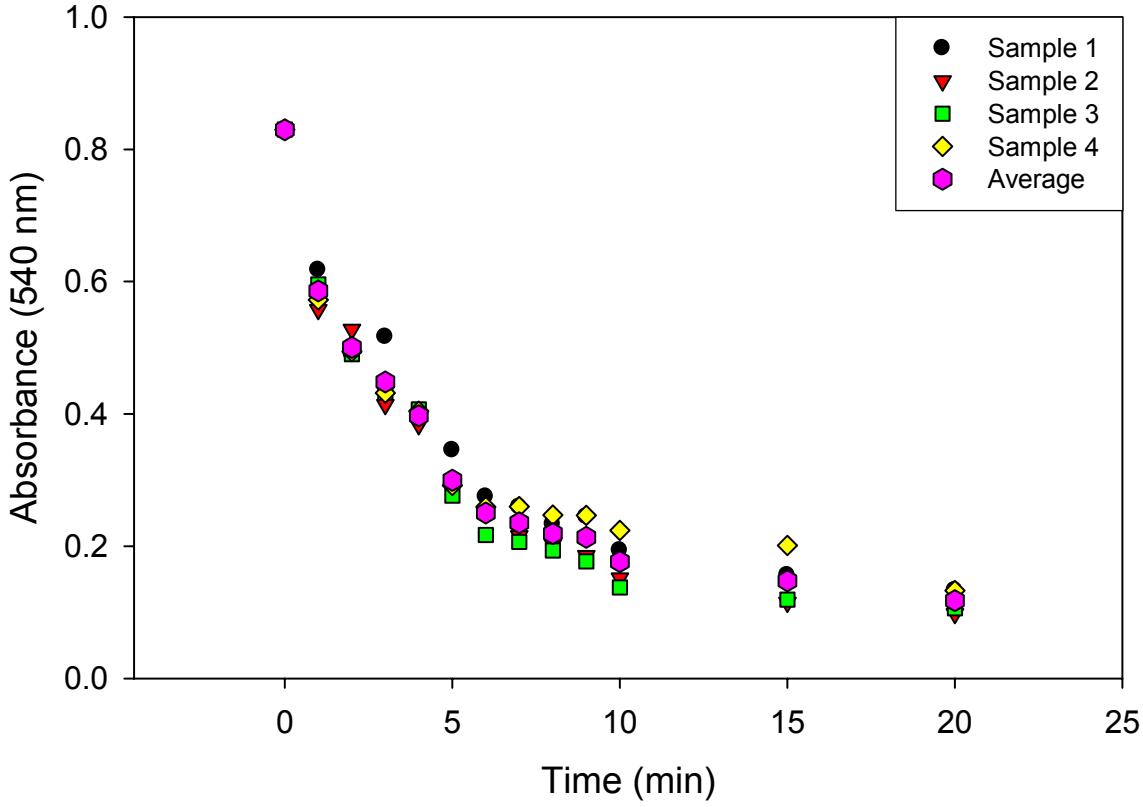

Figure 3.6. Absorbance versus time plots for the multi-sample reactor. The absorbance for each sample of the reactor is plotted, as well as the average.

3.3.2.4. *Effect of pH*

It has been concluded that the AOP of blood must be done at pH 3.0 in order to inhibit catalase present in the blood.[12] Monitoring the process by UV/Vis spectrophotometry has shown that there is a two-step process involved with the decomposition kinetics. This will be presented in detail in a later section. However, the effect of pH will be discussed here. It can be seen in Figure 3.7 that the decomposition of blood begins to level out at approximately 25 min, although the absorbance does not go to zero, indicating an incomplete process. This may be explained by the photo-reduction of ferric ions in the Fenton process, which is the dominant mechanism of •OH production at later times

$$Fe^{3+} + H_2O + h\nu \rightarrow Fe^{2+} + H^+ + \bullet OH \qquad \text{Equation 1.11}$$

According to the La Chatelier's principle, at low pH, the equilibrium will tend to shift toward the reactant side. Therefore, less •OH will be produced. To overcome this, the pH needs to be adjusted to a basic pH so that more •OH will be generated. A pH of 9.0 was chosen early in the blood AOP development because studies showed more complete oxidation of Cr(III) to Cr(VI) at pH 9.5.[13,14] The pH could not be adjusted until after 40 min of UV irradiation at pH 3.0 due to reversible inhibition of catalase. If KOH is added before this time, foaming will occur. After 40 min, the catalase becomes irreversibly inhibited, and base can be added.

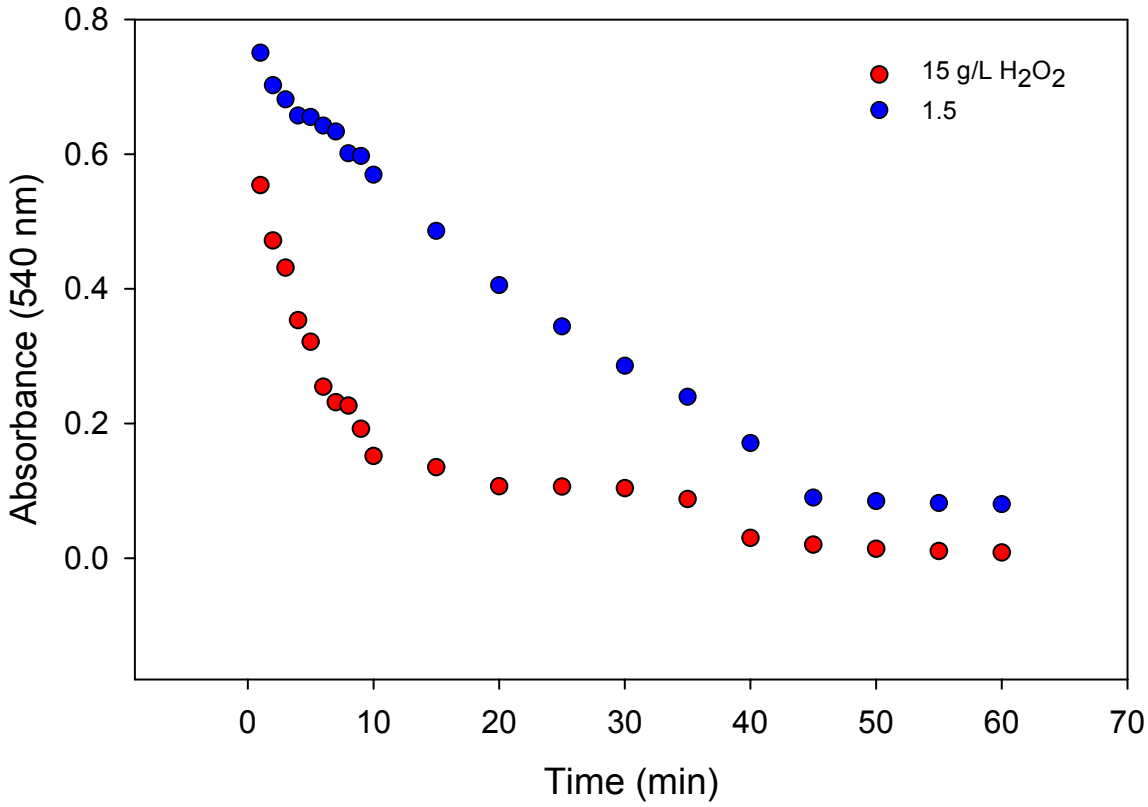

Figure 3.7. Absorbance versus time plots for 2-step AOP process. The first 40 min of the AOP process are performed at pH 3, while the 20 min are done at pH 9.5. The red plot is 15 g/L H_2O_2 and the blue plot is 1.5 g/L H_2O_2.

Once the pH was adjusted with KOH, the UV irradiation was continued and the AOP process was again monitored by UV/Vis. Another slope indicating decomposition of blood is seen for 40–60 min AOP time in Figure 3.7. It is in this time-frame that the blood is almost completely decomposed and the absorbance approaches zero.

3.3.2.5. *Excess H_2O_2*

After the entire 60-min AOP of blood, excess H_2O_2 is present. Titrations were done to determine the amount of H_2O_2 used during the AOP process with different concentrations of H_2O_2. The results of these experiments (Tables 3.1 and 3.2) confirm that there is excess H_2O_2 in the process, which allows pseudo-first order kinetics to be assigned (discussed later). However, the results suggest that only 15-25% of the total H_2O_2 is used during the entire process. This contradicts the UV/Vis experiments. While it is believed there is an excess of H_2O_2, these results are higher than expected. False, high H_2O_2 concentrations may be due to interferences present in the blood that may also reduce MnO_4^- to Mn(II) during the titration. Fe^{3+} is the most likely interferent. Therefore, precise values of the excess H_2O_2 cannot be determined. Explanation for the excess H_2O_2 should be addressed, however. Perhaps this is due to the recombination of •OH to form H_2O_2.

3.3.3. Kinetic Order with Respect to H_2O_2

There are three challenges in studying the kinetics of the Advanced Oxidation Process of blood by H_2O_2. First, blood is a very complex matrix, and cannot be evaluated as simply as an AOP system containing only one component. Second, a typical UV lamp gives the irradiation in a variety of wavelengths, and rates of the photochemical reactions at different wavelengths may be different. Three, $Fe^{2/3+}$ ions released from the AOP of blood samples play the role of a catalyst. Thus this is an autocatalytic process with complex kinetics.

In addition, both blood and H_2O_2 absorb strongly in the UV range, as shown in Figures 3.2 and 3.3. Blood can potentially be decomposed by both direct UV irradiation and •OH radicals produced by the UV irradiation of H_2O_2, two parallel pathways. Control studies using blood solutions containing no H_2O_2 (Figure 3.8), however, revealed that the decomposition of blood by direct UV irradiation is negligible. The dominant pathway is thus the decomposition by •OH radicals.

The interaction of H_2O_2 with the UV light and decomposition of blood is a consecutive reaction that involves at least two major steps: (1) photochemical reaction to generate the •OH radicals; (2) reactions of the •OH radicals with blood to decompose the latter (Equation 3.5).

$$H_2O_2 \xrightarrow{h\nu} 2\ \bullet OH \xrightarrow{\text{blood}} CO_2 + H_2O + \text{inorganic species} \qquad \text{Equation 3.5}$$

Table 3.1. Results of titrations of H_2O_2 with $KMnO_4$ to determine excess H_2O_2.

15 g/L H_2O_2	**before AOP**	**after AOP**	**difference**	**% used**
H_2O_2 in H_2O 40 min AOP	16.0	10.7	5.3	33.1
H_2O_2 in blood (40 min AOP)	16.0	12.0	4	25.0
8.3 g/L H_2O_2	**before AOP**	**after AOP**	**difference**	**% used**
H_2O_2 in H_2O 40 min AOP	9.0	5.8	3.2	35.6
H_2O_2 in blood (40 min AOP)	9.0	6.6	2.4	26.7
3.0 g/L H_2O_2	**before AOP**	**after AOP**	**difference**	**% used**
H_2O_2 in H_2O 40 min AOP	3.7	2.1	1.6	43.2
H_2O_2 in blood (40 min AOP)	3.7	3.0	0.7	18.9
1.5 g/L H_2O_2	**before AOP**	**after AOP**	**difference**	**% used**
H_2O_2 in H_2O 40 min AOP	2.0	1.1	0.9	45.0
H_2O_2 in blood (40 min AOP)	2.0	1.7	0.3	15.0
Average % H_2O_2 used (water, AOP 40 min)		39.2%	±5.8	
Average % H_2O_2 used (blood, AOP 40 min)		21.4%	±5.4	

Table 3.2. Control titrations for the determination of excess H_2O_2 in AOP samples.

H_2O_2 in H_2O (no UV)	**[H_2O_2] g/L**
15 g/L H_2O_2	14.9
8.3 g/L H_2O_2	8.5
3.0 g/L H_2O_2	3.3
1.5 g/L H_2O_2	1.8
Blood Only (no UV, no H_2O_2)	0.2
Fenton (blood only, UV 40 min)	0.6

The light absorption by H_2O_2 is very strong. The photon flux by a 5.5-W UV lamp is small, and a major portion of the photons is absorbed by blood. If the concentration of H_2O_2 is high, and the absorption by water in the UV region is ignored, the limiting reagent is the photon flux of the UV light.[11] Such photochemical reactions follow zeroth-order kinetics. The subsequent radical reactions between the •OH radicals and the components in blood are usually fast. The rate determination step is thus the photochemical reaction of H_2O_2 with the UV light.

When the concentration of H_2O_2 is low, and the main absorber of the UV irradiation is the water background (and blood in the current case), the limiting reagent is H_2O_2 itself, and the photochemical reaction follows the first-order kinetics with respect to $[H_2O_2]$.[11]

It is not clear what the order (x) of the photochemical reaction is with respect to $[H_2O_2]$ in the AOP of blood using H_2O_2 and UV irradiation (Equation 3.6).

$$Rate = k\,[H_2O_2]^x \qquad \text{Equation 3.6}$$

It is also important to understand the complexity of the blood matrix. At any given time of the AOP process, numerous compounds within the blood could be decomposing. It is impossible to account for and study the rate of decomposition of each component in the blood. A decrease in absorbance indicates the decomposition of an unknown number of organic species in the blood. Therefore, in these experiments, and for the sake of simplicity, the blood is

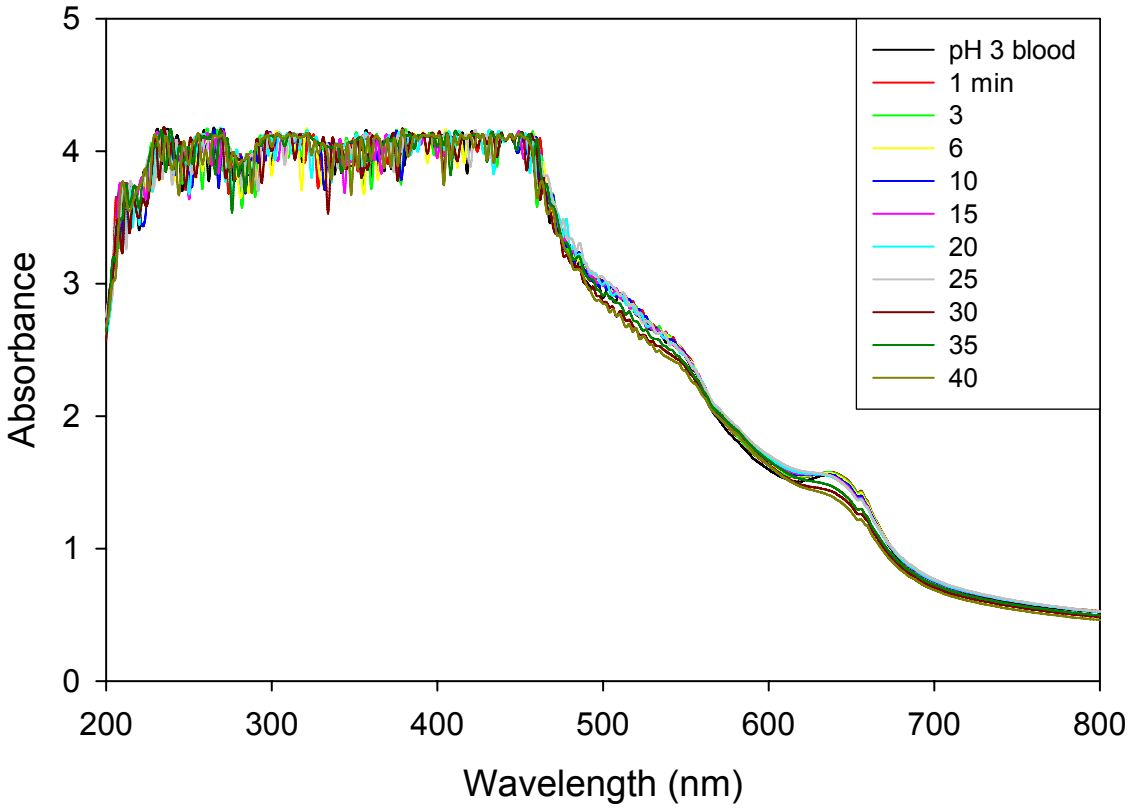

Figure 3.8. UV/Vis spectra of degradation of blood by UV photolysis only. Spectra were taken during different time intervals of UV irradiation. No H_2O_2 was added to the samples. The data indicates a very small decrease in absorbance during the course of the experiments.

assumed to be one absorbing species. The absorbance is assumed to be the collective absorbance of all the components of the blood and is therefore proportional to the concentration of blood. If the components in a blood sample are treated as a "single component," the overall kinetic law is given in Equation 3.7.

$$d\,[\text{blood}] / dt = Rate = k\,[H_2O_2]^x \qquad \text{Equation 3.7}$$

When H_2O_2 is in excess, as in the current work, $[H_2O_2]$ is treated as a constant. Thus

$$d\,[\text{blood}] / dt = k\,[H_2O_2]^x = k' \qquad \text{Equation 3.8}$$

$$1 - ([\text{blood}]_t / [\text{blood}]_0) = (k' / [\text{blood}]_0)\, t \qquad \text{Equation 3.9}$$

$$1 - (A_t / A_0) = k''\, t \qquad \text{Equation 3.10}$$

where A_t and A_0 are the absorbance of the blood at t and $t = 0$, respectively, and $k'' = k' / [\text{blood}]_0 = k\,[H_2O_2]^x / [\text{blood}]_0$.

The plots of absorbance versus time in Figure 3.5 suggest that there is a two-step process involved in the AOP of blood. Such two-step processes have been reported elsewhere.[10,15-16] This is rationalized by a fast initial rate when

Fe^{2+} ions dominates in the Fenton portion of the reaction, and a second, slower step due to much slower reaction of Fe^{3+} ions with H_2O_2.[15,16]

The *approximate* kinetic order *x* with respect to H_2O_2 in the first step, when 82% of the blood decomposition occurs, were determined. Data from several runs using different $[H_2O_2]$ were processed using Equation 3.10, giving the kinetic plot in Figure 3.9. The slopes of these plots (*k*" values) are summarized in Table 3.3.

A plot of ln *k*" verses ln $[H_2O_2]$ (Figure 3.10) yielded the order $x = 0.27$, suggesting the order of the photochemical reaction with respect to H_2O_2 is between the zeroth and first order.

It has also been shown that the concentration of total organic carbon (TOC) in an AOP system has an effect on the kinetic rate of carbon loss, or decomposition. Sigman *et al.* found that a solution containing high TOC (13,000 ppm) did not follow a zero-order rate. They attributed this variation in the photolytic system to the complete consumption of •OH radicals by the organic species. In solutions with lower TOC, they believe •OH radicals formed by photolysis continue to react with intermediate oxidation products from the organic species, further assisting in the total decomposition.[1]

3.4. CONCLUDING REMARKS

The decomposition of blood by the advanced oxidation process has been studied. The process is a combination of three advanced oxidation

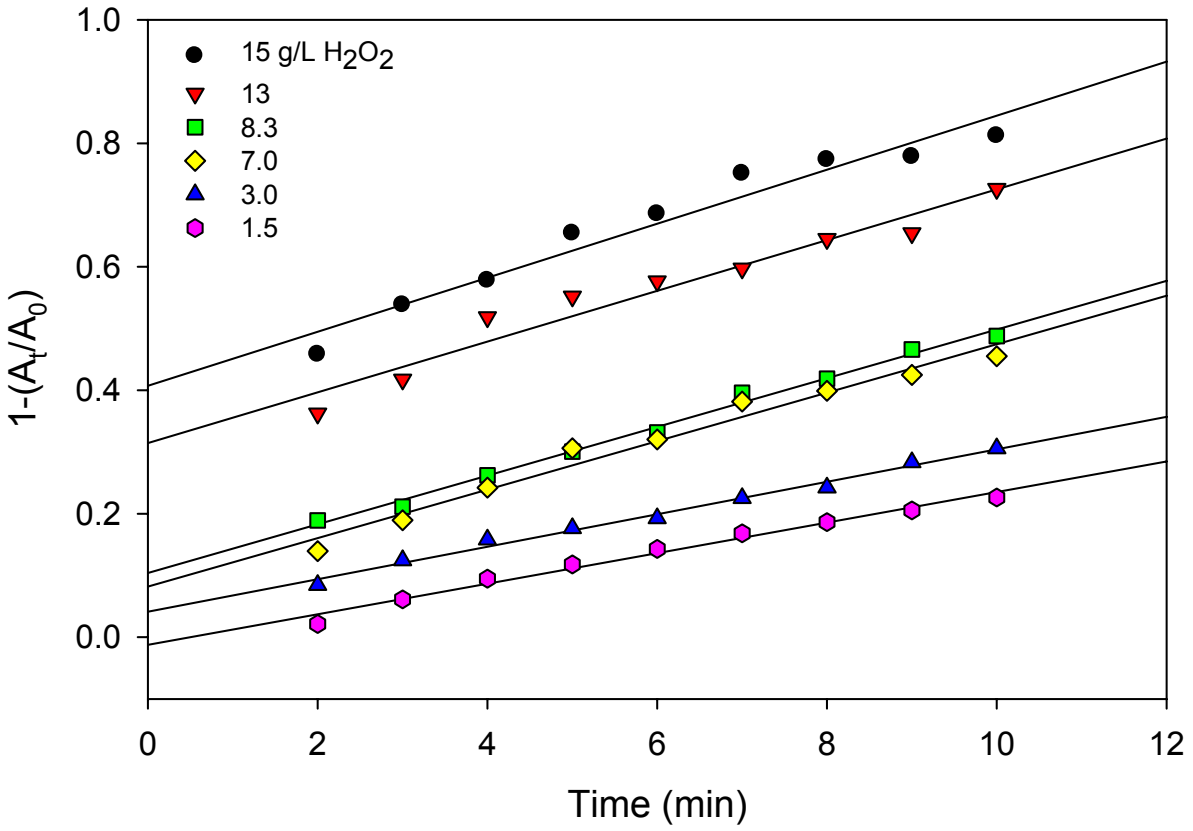

Figure 3.9. Kinetic plots of AOP for different concentrations of H_2O_2 based on the process being zero-order in respect to blood. Slopes of the plots are *k*''.

Table 3.3. *k*" values at different $[H_2O_2]$.

$[H_2O_2]$ (g/L)	*k*''	R^2
1.5	0.0248	0.985
3.0	0.0263	0.990
7.0	0.0393	0.974
8.3	0.0394	0.993
13	0.0411	0.950
15	0.0437	0.953

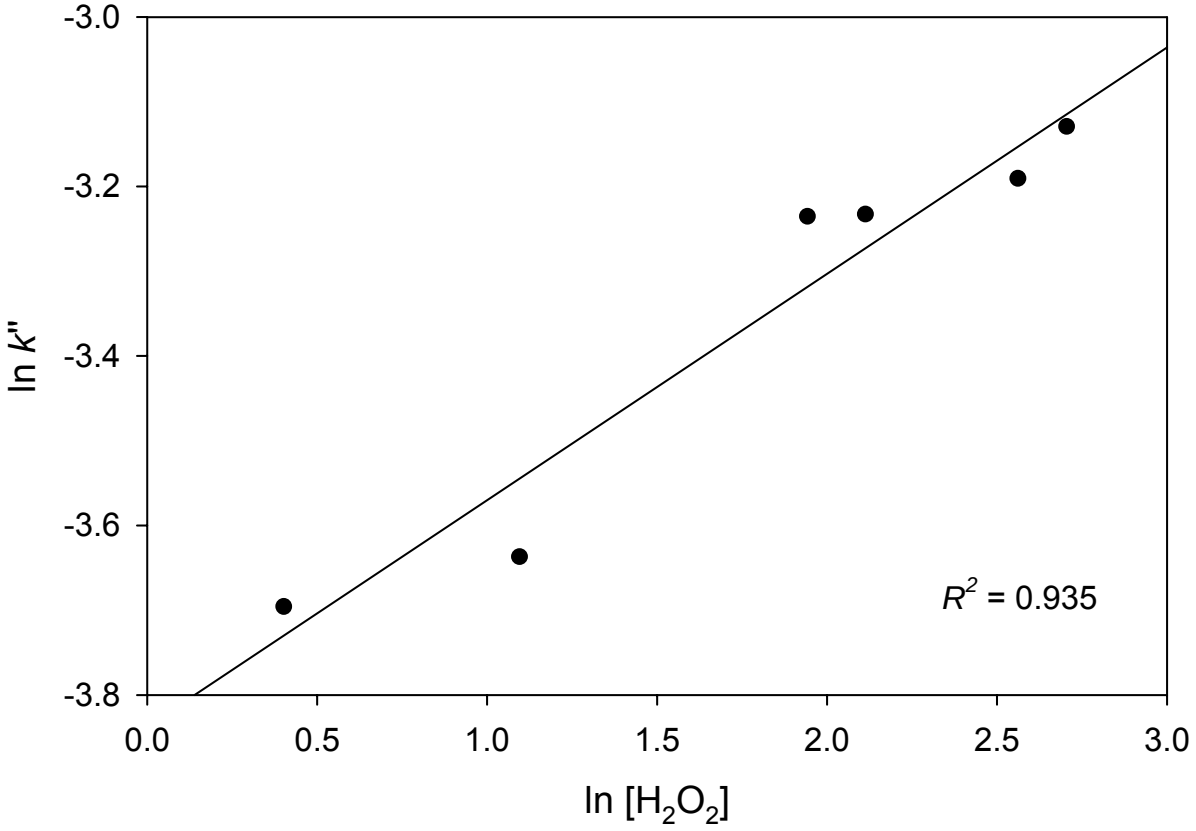

Figure 3.10. Plots of ln (*k*'') versus ln [H_2O_2] based on the data from Figure 3.9. The slope of the line, 0.27, is the order of AOP reaction with respect to H_2O_2.

processes, photolysis of H_2O_2 by UV light, a Fenton process that produces hydroxyl radicals through the series of reactions involving biological ferrous ions and H_2O_2, and a photo-reduction of aqueous ferric ions by UV light. It was determined that there are two steps in the process, indicated by two slopes on the plot of absorbance versus time. A change in the pH after the first 40 min allows for further decomposition of the blood. This study has given an insight into the processes which take place during the advanced oxidation process of blood.

REFERENCES

(1) Sigman, M. E.; Buchanan III, A. C.; Smith, S. M. *J. Adv. Oxid. Technol.* **1997**, *2*, 415.

(2) Alshamsi, F. A.; Albadwawi, A. S.; Alnuaimi, M. M.; Rauf, M. A.; Ashraf, S. S. *Dyes Pigments* **2007**, *74*, 283-287.

(3) Kavitha, V.; Palanivelu, K. *J. Photochem. Photobiol., A* **2005**, *170*, 83-95.

(4) Zhang, W.; Xiao, X.; An, T.; Song, Z.; Fu, J.; Sheng, G.; Cui, M. *J. Chem. Technol. Biotechnol.* **2003**, *78*, 788-794.

(5) Shemer, H.; Kunukcu, Y. K.; Linden, K. G. *Chemosphere* **2006**, *63*, 269-276.

(6) Zimbron, J. A.; Reardon, K. F. *Water Res.* **2005**, *39*, 865-869.

(7) Benitez, F. J.; Real, F. J.; Acero, J. L.; Leal, A. I.; Cotilla, S. *J. Environ. Sci. Health, Part A* **2005**, *40*, 2153-2169.

(8) Schumb, W. C.; Satterfield, C. N.; Wentworth, R. L. *Hydrogen Peroxide*; Reinhold Publishing: New York, 1955.

(9) Ntampegliotis, K.; Riga, A.; Karayannis, V.; Bontozoglou, V.; Papapolymerou, G. *J. Hazard. Mater.* **2006**, *136*, 75-84.

(10) Benitez, F. J.; Real, F. J.; Acero, J. L.; Garcia, C.; Llanos, E. M. *J. Chem. Technol. Biotechnol.* **2007**, *82*, 65-73.

(11) Stephan, M. I. in *Advanced Oxidation Processes for Water and Wastewater Treatmen,* Parsons, S., Ed., IWA Publishing: London, 2004, p. 7.

(12) Yong, L.; Armstrong, K. C.; Dansby-Sparks, R. N.; Carrington, N. A.; Chambers, J. Q.; Xue, Z.-L. *Anal. Chem.* **2006**, *78*, 7582-7587.

(13) Rodman, D. L.; Carrington, N. A.; Xue, Z. L. *Talanta* **2006**, *70*, 668-675.

(14) Rodman, D. L., Ph.D. dissertation, The University of Tennessee, Knoxville, 2005.

(15) Kwan, C. Y.; Chu, W. *Wat. Res.* **2003**, *37*, 4405-4412.

(16) Kwon, B. G.; Lee, D. S.; Kang, N.; Yoon, J. *Wat. Res.* **1999**, *33*, 2110-2118.

Part 4

Design and Characterization of a Bismuth Bulk Electrode

4.1. INTRODUCTION

A BiBE was designed and fabricated as an alternative for a BiFE for the detection of trace levels of Cr(VI). As previously discussed, BiFE have become desirable for many measurements typically performed at both hanging mercury drop electrodes (HMDE) and mercury film electrodes (MFE). The BiFE is plated *in situ* or *ex situ* onto a substrate electrode, such as glassy carbon. Experiments with the BiFE proved to have challenging issues with film formation and measurement irreproducibility. The thought behind the BiBE is that the surface of the electrode would remain the same from experiment to experiment, and therefore, results would be more reproducible. The in-house fabricated electrode was found to be especially useful for the study of the electrochemical mechanism of DTPA binding with chromium and the bismuth surface. The results from the experiments with the BiBE are discussed.

4.2. EXPERIMENTAL

4.2.1. Instrumentation

All voltammetric measurements were performed using a modulated CHI 440 potentiostat (CH Instruments). A three-electrode configuration consisted of a bulk bismuth (BiBE) disk working electrode (0.8 mm diameter), Ag/AgCl reference electrode, and a platinum wire counter electrode. The BiBE was made in-house by melting bismuth needles (99.998% purity, Alfa Aesar) into a hand-

blown glass casing. The melting process was done by placing several rods of bismuth into the glass casing. A tin-coated copper wire was inserted partially into the glass casing such that the bismuth would melt around it and would act as the electrical lead. This ensemble was vertically inserted into a glass tube, which was then sealed and connected to a vacuum line. The air from the tube was removed by vacuum and nitrogen was pumped in. The tube was held over a Bunsen burner until the bismuth was melted completely (melting point: 271.3 °C). After cooling, the electrode was removed from the tubing, and the end serving as the surface of the electrode was cut with a diamond band saw. The freshly exposed electrode surface was smoothed by polishing with a series of emery paper of 200, 400, 600, and 800 grit. Further polishing was done using a standard electrode polishing kit (CH Instruments) that includes a 1200 grit Carbimet disk, 1.0 μm alumina slurry on a nylon cloth, 0.3 μm alumina slurry on a nylon cloth, and 0.05 μm alumina slurry on a Microcloth polishing pad. The images in Figure 4.1 are a schematic and pictures of the BiBE and its surface.

4.2.2. Reagents

Potassium nitrate (Certified ACS, Fisher), acetic acid (glacial, Fisher), sodium acetate (anhydrous, Certified ACS, Fisher), cadmium acetate (Certified ACS, Fisher), and diethylenetriaminepentaacetic acid (DTPA, ≥99%, Fluka) were used as received. Cr(VI) AA standard solution (1000 mg/L, Aldrich) was diluted prior to use. The buffer solution contained 0.1 M sodium acetate and 0.25 M KNO_3 and its pH was adjusted to 6.0 with CH_3COOH. The DTPA solution (0.1

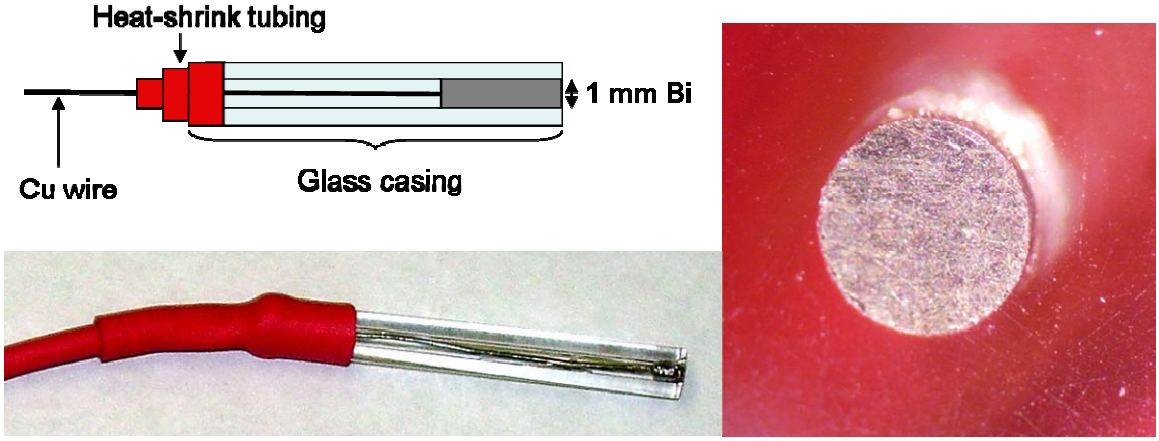

Figure 4.1. Bismuth bulk electrode: schematic diagram, electrode picture, and electrode surface.

M) was prepared by dissolving DTPA in water while slowly adjusting pH to 6.0 with 25% NH_4OH (Fisher Scientific). Cr(VI) standards were prepared by diluting the appropriate amount of stock solution in electrolytes. All aqueous solutions were prepared in 18 MΩ deionized H_2O.

4.2.3. Procedures

The electrode was polished before each use following the method outlined above to ensure fresh bismuth surface. A conditioning step was developed and was found to provide more reproducible results when used immediately after polishing. The electrode was cycled in a 0.1 M acetate buffer solution containing 0.25 M KNO_3^- (pH 6.0). The conditioning step included cycling from 0 to -1.4 (50 scans) with a scan rate of 50 mV/s. A solution of cadmium was measured by CV to determine if the electrode was well conditioned and ready for experiments. It was also found that a conditioning step performed in a 13 ppm Cr(VI) solution resulted in more reproducible Cr(III) to Cr(II) reduction peaks at -1.1 V. If this step was omitted, the above mentioned peak occurred at -1.2 V.

Cyclic Voltammetry (CV) experiments were performed to characterize the Bi electrode and to study its interaction with DTPA, Cr(VI), and Cr(III). The CV was scanned under the same conditions as the conditioning step. A pulsed method, differential normal pulse voltammetry (DNPV), was used to detect trace amounts of Cr(VI). For these experiments, an accumulation step was run by holding the potential at -0.8 V for 180 s followed by a DNPV scan from -0.1 to -1.4 V.

4.3. RESULTS AND DISCUSSION

4.3.1. Characterization of the Bismuth Bulk Electrode

The surface of the BiBE and the electrochemical mechanism of Cr(VI) detection were studied using CV in different solutions Cr(VI), Cr(III), and buffer. The fundamental behavior of the BiBE was observed in 0.1 M acetate buffer at pH 6.0 (Figure 4.2). Important information was obtained from this data. First, the large peak occurring at -0.4 V is due to the reduction of bismuth oxide. The reduction of anodically formed bismuth oxide to metallic bismuth is given in the following reaction:

$$Bi_2O_{3(s)} + 3\ H_2O_{(aq)} + 6\ e^- \rightarrow 2\ Bi_{(s)} + 6\ OH^-_{(aq)} \qquad \text{Equation 4.1}$$

Secondly, the large negative peaks in the range from 0 to -0.2 V are the oxidation of the bismuth.[1] Third, the current begins to increase around -1.35 V as a result of hydrogen evolution. The working potential window for this electrode is from 0 to -1.4 V. At potentials above 0 V, a thicker, irreversible bismuth oxide layer is formed. The shiny surface of the bismuth turns black as a result of the oxidation. The CV in Figure 4.2 is expected each time the electrode is polished and a fresh bismuth surface is exposed. The potential window can be expanded to more negative potentials, up to -1.7 V, if the pH of the electrolyte solution is increased to approximately 13.[2]

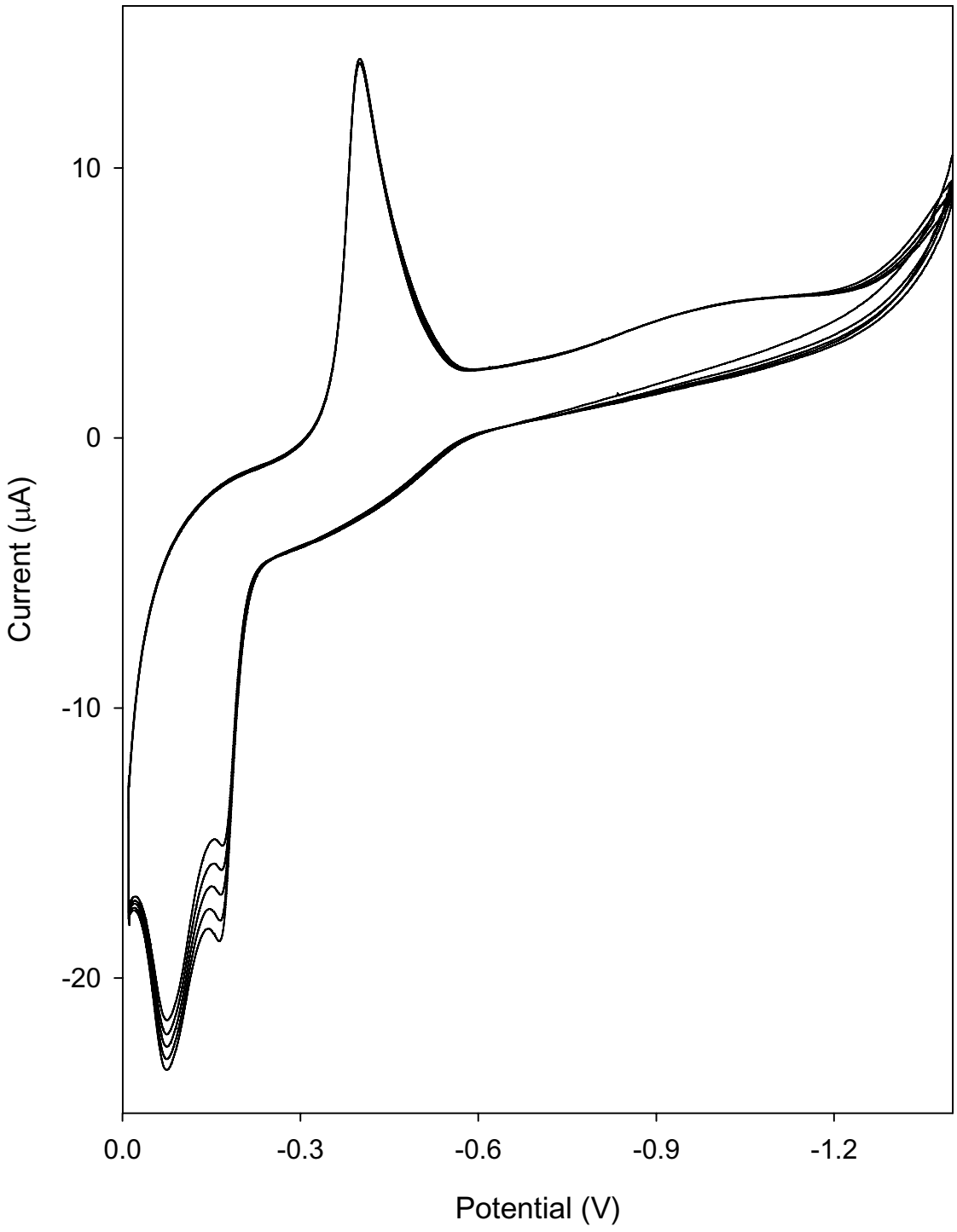

Figure 4.2. CV of BiBE in 0.1 M acetate buffer at pH 6.0. The peak at -0.4 V is the reduction of bismuth oxide, while those peaks from 0 to -0.2 V are the oxidation of bismuth.

A standard method for evaluating the function of an electrode is to measure the redox of ferric-/ferro-cyanide using CV. This redox system could not be used to test the integrity of the BiBE because the potential window of the BiBE is much more negative than the redox potentials of ferric-/ferro-cyanide. However, one redox system that can be used in the BiBE potential range to test its cathodic interfacial properties is Cd(II)/Cd(0).[2] A 100 ppm Cd(II) solution was prepared in 0.1 M acetate buffer containing 0.25 M KNO_3 with a pH of 6.0. CV experiments resulted in voltammograms as in Figure 4.3. The peak at -0.79 V is from the reduction of Cd(II) while the peak at -0.73 V is from the re-oxidation of Cd(0). The peak separation of 60 mV indicates a quasi-reversible process.[2] The rising current past -0.9 V is from the uncatalyzed reduction of nitrate.

4.3.2. Mechanistic Studies of Cr Detection Using DTPA on the Bi Bulk Electrode

The exact role of DTPA in the mechanism of electrochemical Cr(VI) detection (as mentioned in Part 2) was not fully understood. It was unclear if DTPA binds to the surface of the electrode by a physical adsorption or covalent bonding. To better understand the process, experiments similar those of Sander *et al.* were conducted using CV.[3] The mechanism of DTPA binding with Cr(VI) and Cr(III) were examined at a HMDE by Sander and coworkers. In this series of experiments, CV was used to study the electrochemistry of solutions of electrolyte, Cr(III), and Cr(VI) both in the absence and presence of DTPA. Cr(III) and Cr(VI) (0.25 mM) in 0.1 M acetate buffer without nitrate were used.

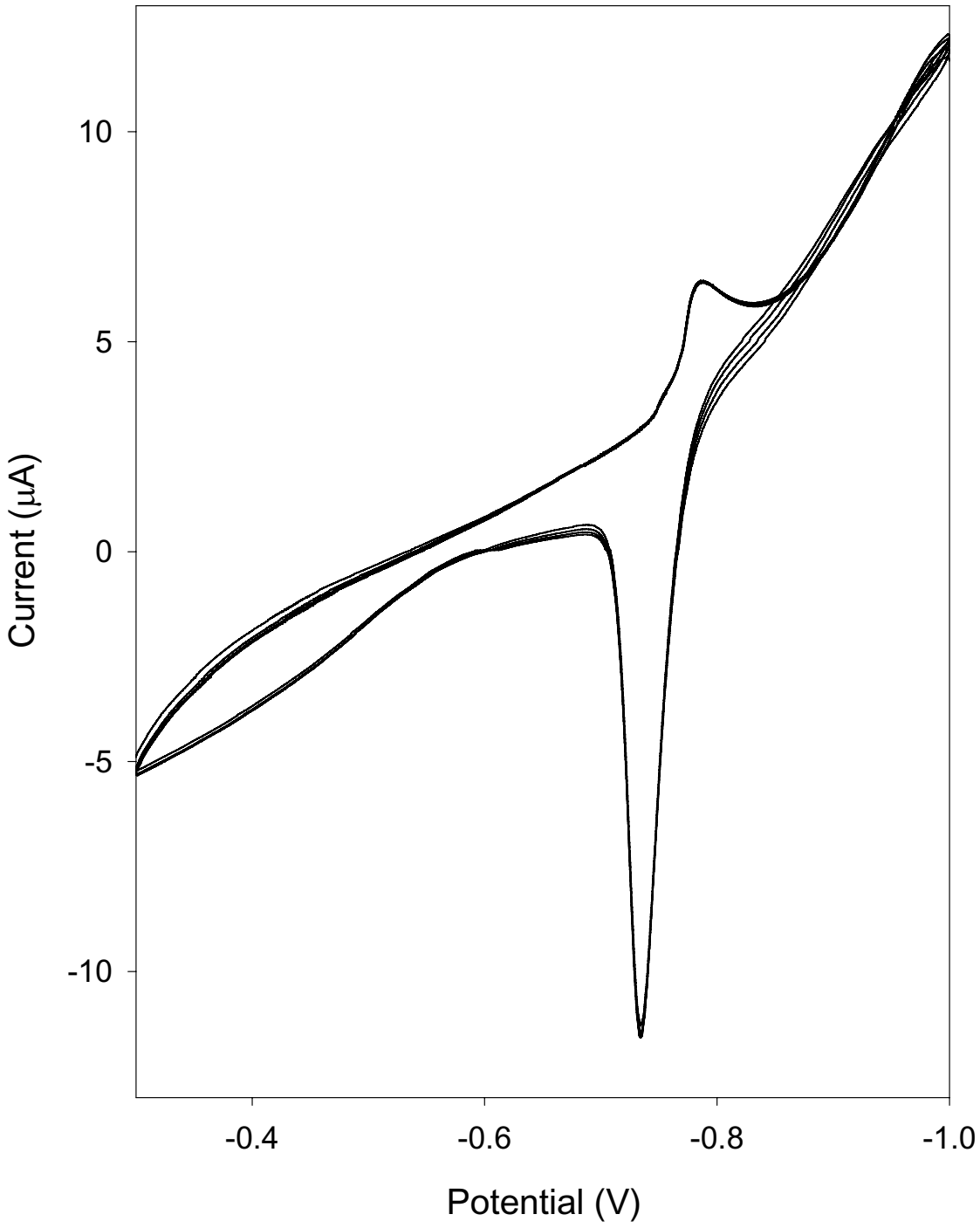

Figure 4.3. CV of Cd(II)/Cd(0) redox couple at the BiBE.

4.3.2.1. DTPA at the BiBE

In Figure 4.4, CVs of acetate buffer without (blue) and with (red) DTPA are shown. The familiar peak at -0.4 V from the reduction of bismuth oxide is present in the scan without DTPA, as well as that of the bismuth oxidation above -0.2 V. When DTPA is added to the solution, the reduction peak at -0.4 V disappears and the oxidation peaks above -0.2 V increase. These observations may suggest the covalent binding of DTPA with the bismuth surface itself.

4.3.2.2. Cr(III) at the BiBE

Behavior of Cr(III) at the BiBE without (blue) and with (red) DTPA are shown in Figure 4.5. The solution of Cr(III) without DTPA exhibits a small peak at -1.35 V, as well as the standard oxidation and reduction peaks attributed to the BiBE. This peak is the reduction of Cr(III) to Cr(II). When DTPA is added, the reduction peak at -0.4 V diminishes. Most noticeably, the peak at -1.35 V is anodically shifted to -1.2 V and the current increases. This peak corresponds to DTPA-Cr(III) being reduced to DTPA-Cr(II).

4.3.2.3. Cr(VI) at the BiBE

CV experiments gave an insight into the interaction of Cr(VI) with DTPA and the BiBE. Figure 4.6 includes voltammograms of Cr(VI) solutions without (blue) and with (red) DTPA. In the scan without DTPA, the typical reduction and oxidation peaks for bismuth oxide and bismuth, respectively. In the scan with only Cr(VI), a small peak around -1.35 V appears due to Cr(III) reduction to Cr(II).

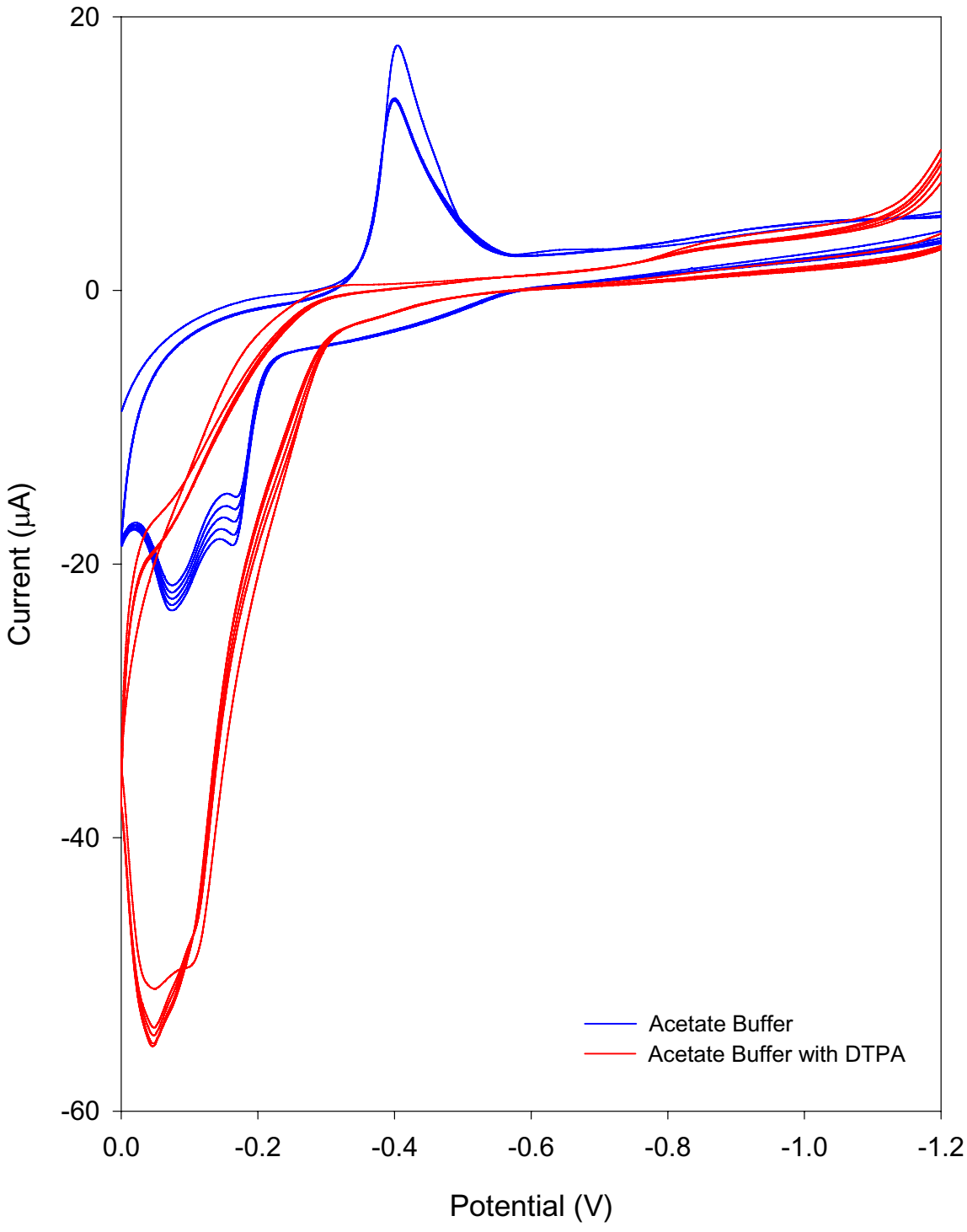

Figure 4.4. CVs of acetate buffer with and without DTPA.

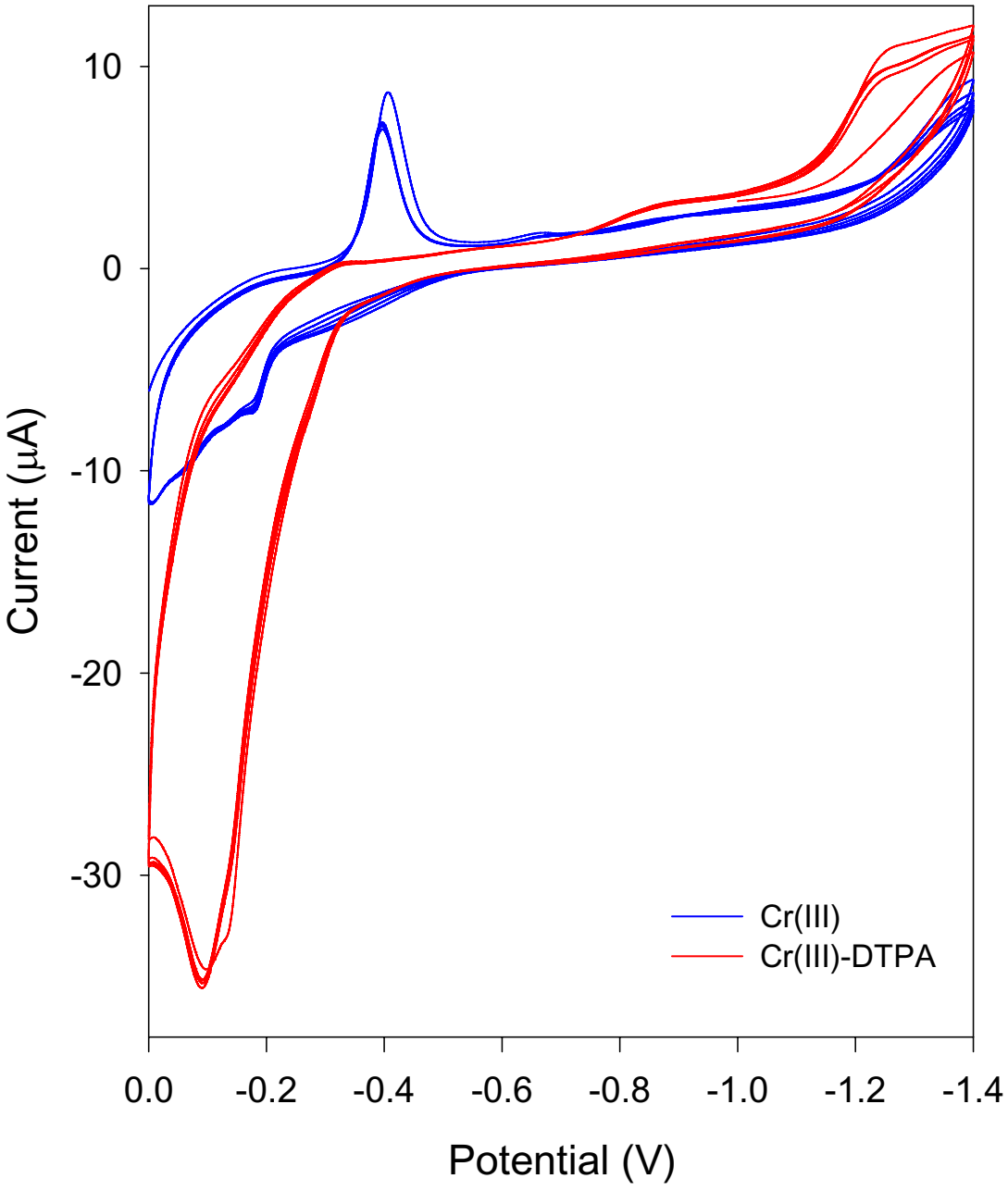

Figure 4.5. CVs of Cr(III) solutions without and with DPTA.

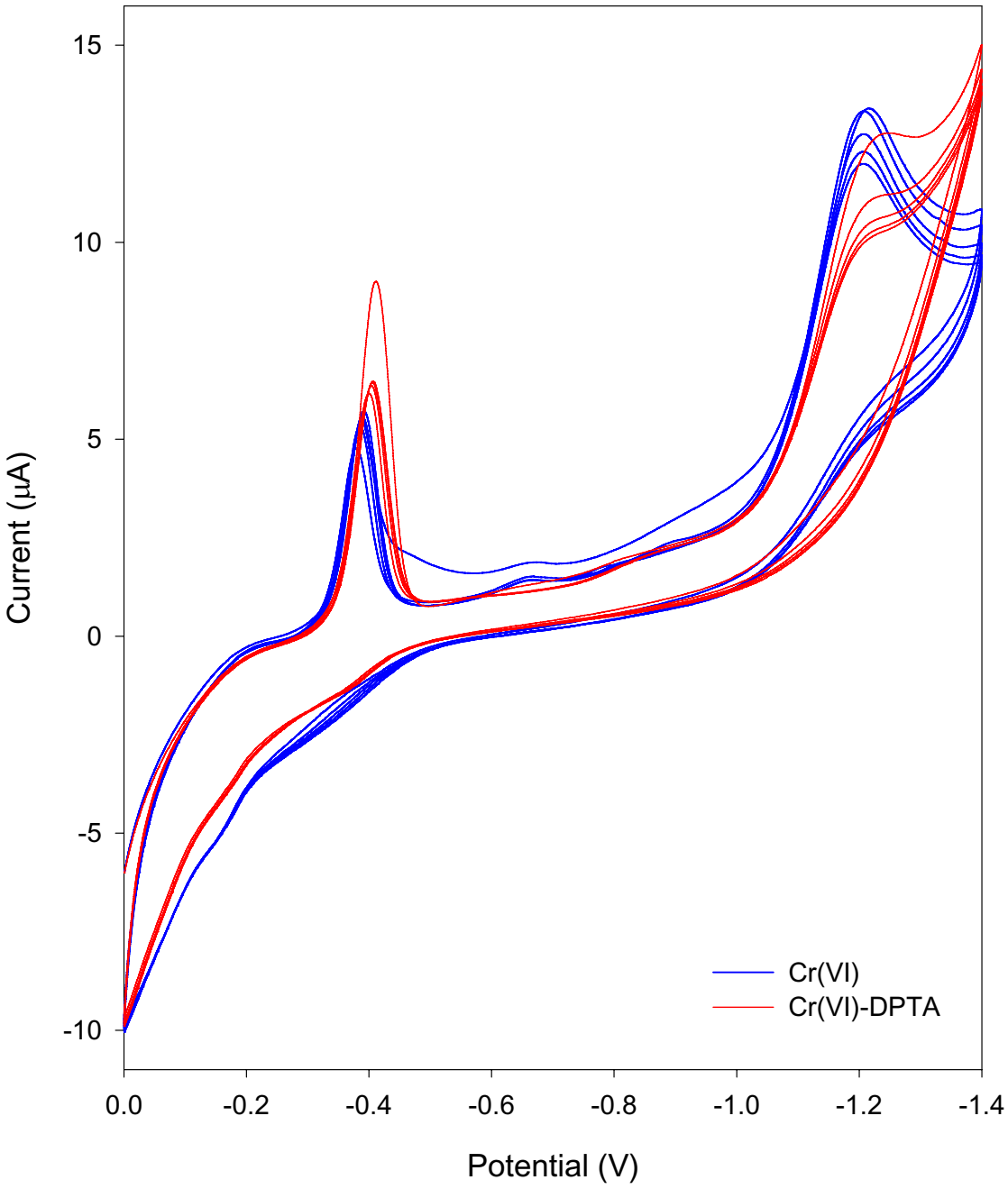

Figure 4.6. CVs of Cr(VI) solutions without and with DTPA.

When DTPA is added to the Cr(VI) solution, an interesting process occurs. The peak at -0.4 V does not disappear as it does with other solutions when DTPA is added. Upon closer inspection, the peak actually shifts cathodically by approximately 10 mV. This suggests that the peak is not from the reduction of bismuth oxide at all, but from the reduction of Cr(VI)-DPTA to Cr(III)-DTPA. The reduction peak at -1.15 V is Cr(III)-DTPA to Cr(II)-DTPA. The difference in the peak currents of the reduction of Cr(III) to Cr(II) without DTPA in Cr(VI) and Cr(III) starting solutions is the electroactivity of the species. Cr(III) in solution exists as a stable hexaquo complex, and is not as electroactive as Cr(VI) because it does not adsorb readily to the electrode surface.[3] Cr(III) freshly reduced from Cr(VI) remains in the double layer and does not rely on diffusion for reduction to Cr(II), therefore generating a higher current.[3] These results are in agreement with similar studies by Sander *et al*. at the HMDE.[3]

4.3.3. Catalytic Adsorptive Stripping Voltammetry at the BiBE

Many experiments were performed on the use of the BiBE for the detection of trace amounts of Cr(VI). The electrochemical procedure followed was that described by Wang *et al*.[4] for the BiFE and used for Cr(VI) detection in blood[5] with nitrate as the oxidant. Disappointingly, the detection of Cr(VI) at ppt or ppb levels was unsuccessful at the BiBE. Two possible explanations for the failure of the electrode are discussed.

4.3.3.1. *Electrocatalyzed Reduction of Nitrate*

The first possible explanation for the inability of the electrode for Cr(VI) detection could be the *catalyzed* reduction of nitrate. For catalytic adsorptive stripping voltammetry at a BiFE, a peak occurred at -1.2 V in solutions blank containing only acetate buffer, nitrate, and DTPA (Figure 2.4). This was believed to be an *uncatalyzed* reduction of nitrate. A recent discussion of the electrocatalytic reduction of nitrate led to a different theory of nitrate reduction in this system. Li *et al.* describe the electrocatalytic reduction of nitrate by a complex of Co(III) with 1,4,8,11-tetraazacyclotetradecane, or cyclam[6] (Figure 4.7A). DTPA (Figure 4.7B) in our system is similar to cyclam in that it contains multiple amine groups. Its exact complexation with transition metals is, however, not known. CV experiments discussed above suggest the binding of DTPA with Bi. It may be possible that the Bi-DTPA acts as a catalyst in the reduction of nitrate, very much like the complex of Co-cyclam. This nitrate reduction peak occurs near the potential where Cr(III) to Cr(II) reduction is expected. The peak is much larger than and dominates the Cr(III) reduction peak (Figure 4.8), thus hindering trace Cr(VI) detection.

4.3.3.2. *Bi Bulk vs. Bi Film Electrodes*

An ongoing study in our research lab on Bi film thickness provide an insight into the lack of success of the BiBE in Cr(VI) detection. The study shows that thinner Bi films are needed for Cr(VI) detection[4] while thicker films are more advantageous for V(V) detection.[7] The V(V) detection requires a thick, blanket

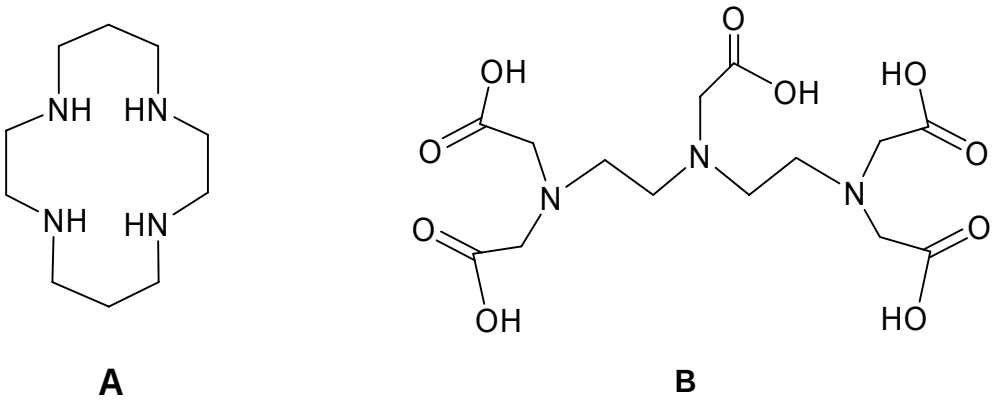

Figure 4.7. Chemical structures of (A) Cyclam and (B) DTPA.

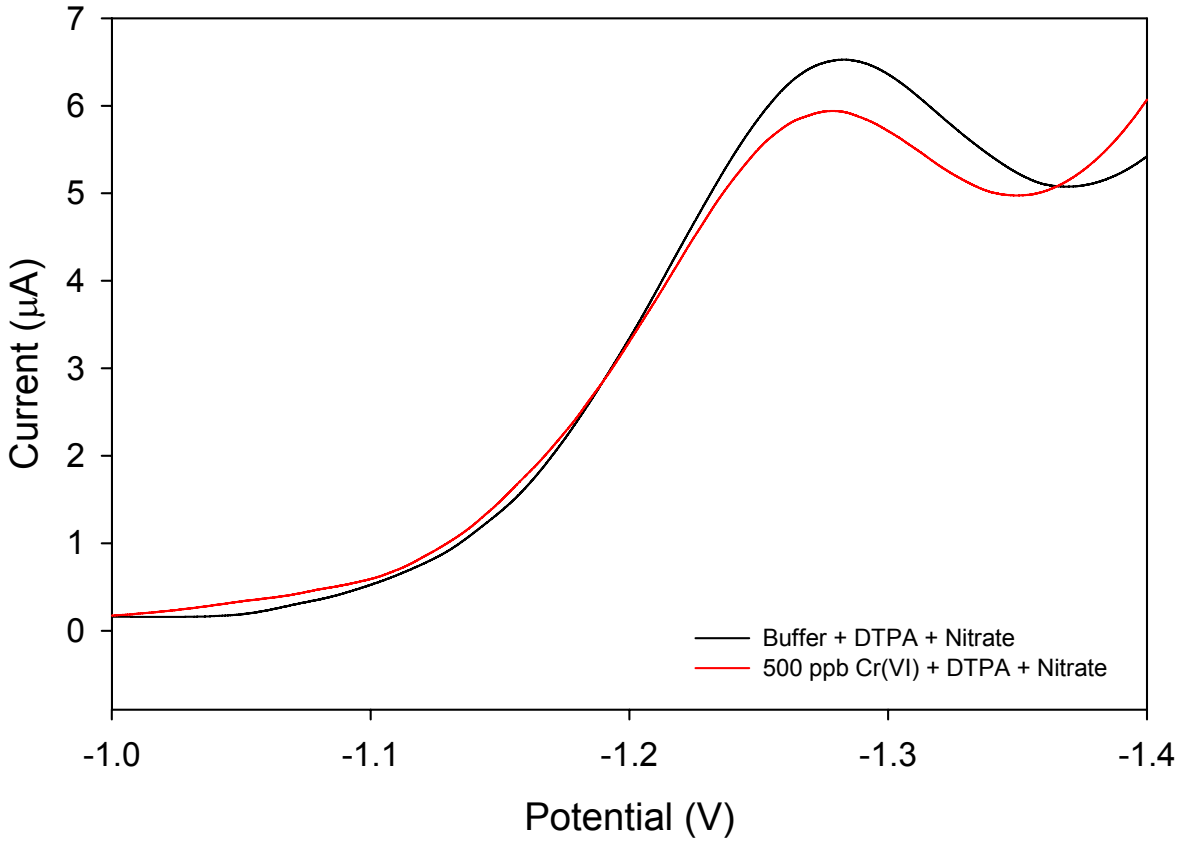

Figure 4.8. SWV of buffer (black) and 500 ppb Cr(VI) (red) in acetate buffer with nitrate and DTPA.

Bi, film which is analogous to the BiBE. The reasoning behind the thin film needed for Cr(VI) detection is unknown at this point. A dependence on the film thickness and its correlation to the BiBE is conjectured. Perhaps the main function of the Bi is to facilitate the electrode process by anchoring DTPA to the substrate interface. The DTPA is then a hook that captures freshly reduced Cr species in the sample. With a Bi film, the reduction of the C(III)-DTPA to Cr(II)-DTPA takes place at the glassy carbon substrate. For the bulk electrode, the entire surface is Bi, which binds to DTPA. It is possible that the surface is covered with DTPA, and electron transfer to the electrode is partially inhibited.

4.4. CONCLUDING REMARKS

The BiBE has been designed and characterized by CV. The information led to a better understanding of the interaction between Bi and DTPA and the binding of DTPA to Cr(VI). However, the bulk electrode did not prove to be useful for the intended purpose of Cr(VI) determination. Another study demonstrating the application of the BiBE for other metal analyses is presented in the next part.

REFERENCES

(1) Grubac, Z.; Metikos-Hukovic, M. *Electrochim. Acta* **1999**, *44*, 4559-4571.

(2) Pauliukaite, R.; Hocevar, S. B.; Ogorevc, B.; Wang, J. *Electroanal.* **2004**, *16*, 719-723.

(3) Sander, S.; Navratil, T.; Novotny, L. *Electroanal.* **2003**, *15*, 1513-1521.

(4) Lin, L.; Lawrence, N. S.; Thongngamdee, S.; Wang, J.; Lin, Y. H. *Talanta* **2005**, *65*, 144-148.

(5) Yong, L.; Armstrong, K. C.; Dansby-Sparks, R. N.; Carrington, N. A.; Chambers, J. Q.; Xue, Z.-L. *Anal. Chem.* **2006**, *78*, 7582-7587.

(6) Li, H.-L.; Anderson, W. C.; Chambers, J. Q.; Hobbs, D. T. *Inorg. Chem.* **1989**, *28*, 863-868.

(7) Wang, J.; Lu, D.; Thongngamdee, S.; Lin, Y.; Sadik, O. A. *Talanta* **2006**, *69*, 914-917.

Part 5

Simultaneous Determination of Lead(II), Cadmium(II), and Zinc(II) by Anodic Stripping Voltammetry at the Bismuth Bulk Electrode

5.1. INTRODUCTION

The bismuth bulk electrode (BIBE) was investigated as an alternative electrode material for the anodic stripping voltammetric analysis (ASV) of Pb(II), Cd(II), and Zn(II). Traditionally, hanging mercury drop electrodes (HMDE) and mercury film electrodes (MFE) have been used for heavy metal analyses by ASV due to their ability to form amalgams with the metals and their negative potential windows.[1] More recently, different electrode materials have been explored for ASV detection of metal species including bismuth film electrodes,[2-5] bismuth-modified carbon paste electrodes,[6] gold-coated diamond thin-film electrodes,[7] and boron-doped diamond electrodes.[8] Metal species detected include arsenic(III),[7] lead(II),[3,8,9] zinc(II),[8] cadmium(II),[3,8-10] thallium(II),[2,3] copper(II),[3] tin(II),[4,5] manganese(II),[6] and cobalt(II).[10] Most detection limits of these metals are in the low ppb range. The use of a BiBE for the simultaneous detection of metal species is described.

5.2. EXPERIMENTAL

5.2.1. Apparatus

Voltammetric experiments were performed using a CH Instruments 440 potentiostat. A three-electrode configuration consisted of a bulk bismuth (BiBE) disk working electrode (3.0 mm or 0.8 mm diameter), a Ag/AgCl reference electrode, and a platinum wire counter electrode. The 0.8 mm BiBE was made in-

house by melting bismuth needles (99.998% purity, Alfa Aesar) into a hand-blown glass casing, as described in Part 4. The 3.0 mm BiBE was made in a similar fashion, except in an open-air environment rather than in nitrogen. The same polishing procedure as described earlier was used for these experiments.

5.2.2. Reagents

Acetic acid (glacial, Fisher), sodium acetate (anhydrous, Certified ACS, Fisher), cadmium acetate (Certified ACS, Fisher), and lead nitrate (Certified ACS, Fisher) were used as received. Zn(II) AA standard solution (1000 mg/L, Aldrich) was diluted prior to use. The buffer solution contained 0.1 M sodium acetate and its pH was adjusted to 6.0 with CH_3COOH. Pb(II), Cd(II), and Zn(II) standards (10-100 ppb) were prepared by diluting the appropriate amount of stock solution in electrolytes. All aqueous solutions were prepared in 18 MΩ deionized H_2O.

5.2.3. Adsorptive Stripping Voltammetry of Pb(II), Cd(II), and Zn(II)

For ASV experiments, 20 mL of standard solutions were used. No deaeration of the samples was required. Square wave voltammetry (SWV) was used for both the accumulation and stripping steps with the following parameters: initial *E*, -1.4 V; final *E*, -0.3 V; increasing *E*, 4 mV; amplitude, 25 mV; frequency, 15 Hz; and quiet time, 240 s. A quiet time of 240 s was used for the accumulation step, during which time the solution was stirred at approximately 1200 rpms. The potential is held constant at the initial potential during the entire

quiet time. The SWV starts immediately upon completion of the quiet time. No resting period was used between the accumulation and stripping steps. Stirring at high speed was required during the accumulation process. The stirring was stopped at the end of the quiet period for the stripping step.

5.3. RESULTS AND DISCUSSION

5.3.1. Simultaneous Determination of Pb(II), Cd(II), and Zn(II)

Simultaneous determination of the metals was performed by making standards containing all three metals. ASV resulted in voltammograms containing three peaks corresponding to the oxidation of Pb(II), Cd(II), and Zn(II). Figure 5.1 is a voltammogram of a mixture of Pb(II), Cd(II), and Zn(II). The peaks were assigned to each metal by spiking. Peaks are Pb(II) (-0.50 V), Cd(II) (-0.75 V), and Zn(II) (-1.10 V), and are in agreement to values in literature.[11] Calibration plots were made for each metal in the mixture (Figure 5.2) to compare with those of the individual metal analyses. These results are listed in Table 5.1.

Different accumulation times were tested for optimal peak formation. For the 3 mm electrode, a 180 s accumulation time was found to be best. At times lower than this, peak heights were lower; at longer accumulation times, the peaks became distorted, possibly due to saturation of the electrode. The 0.8 mm electrode required 240 s for accumulation to produce the largest peaks. Again, results for shorter and longer accumulation times were comparable to those of

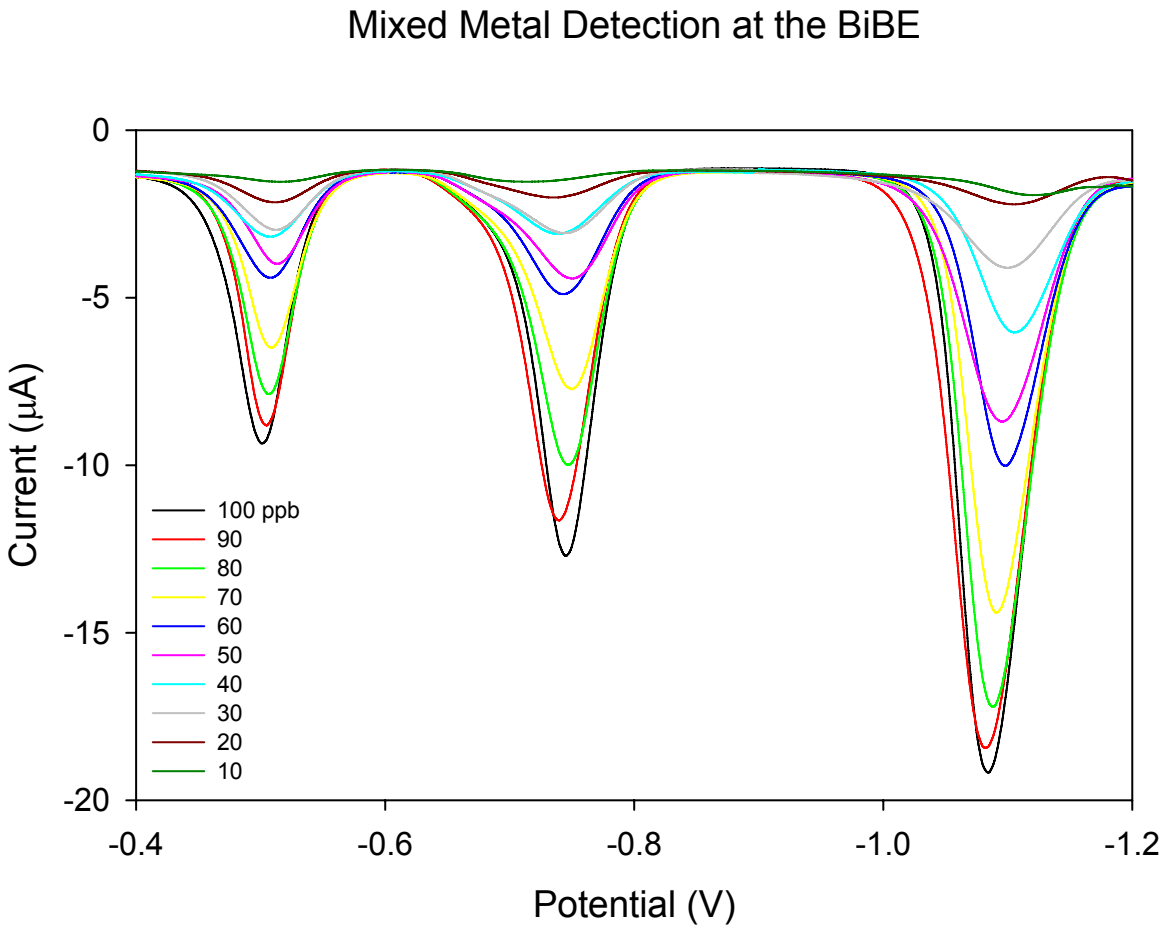

Figure 5.1. ASV calibration of mixed metals. The solutions ranged from 10 to 100 ppb and contained Pb(II) (-0.5 V), Cd(II) (-0.75 V), and Zn(II) (-1.10 V).

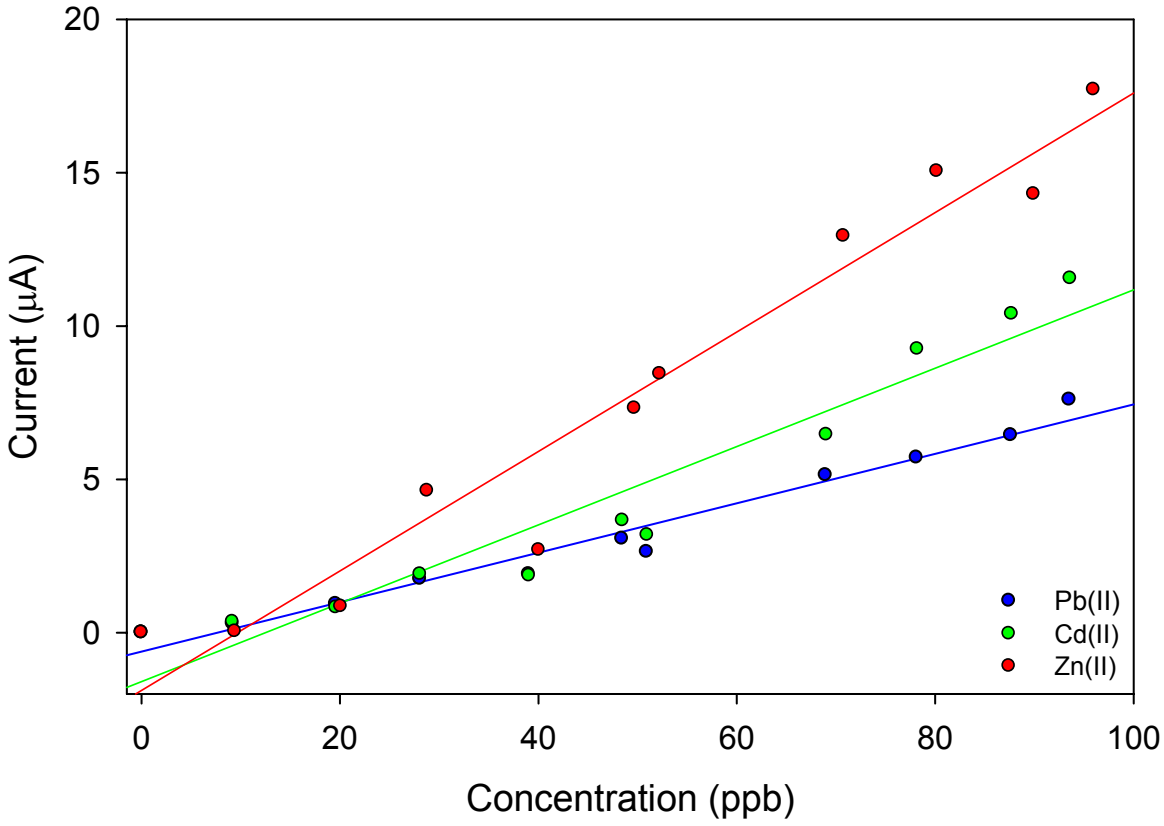

Figure 5.2. Calibration plot of ASV of metals, Pb(II) (blue), Cd(II) (green), and Zn(II) (red), detected simultaneously at the BiBE.

Table 5.1. Comparison of calibration plots for individual and simultaneous metal ASV detection (current versus concentration).

Individual	E_{peak}	R^2	**Slope**
Pb(II)	-0.50	0.973	0.085
Cd(II)	-0.75	0.942	0.128
Zn(II)	-1.10	0.954	0.195
Simultaneous	E_{peak}	R^2	**Slope**
Pb(II)	-0.50	0.975	0.071
Cd(II)	-0.75	0.987	0.099
Zn(II)	-1.10	0.953	0.186

the 3 mm electrode. Stirring was another important issue that was studied. Slow stirring resulted in much smaller peaks than stirring at full speed. This is due to the increased convective mass transport to the electrode surface. Another parameter that was found to be important was starting the SWV immediately after the accumulation step. If a rest period with a constant potential was used, which is often a step in ASV, the peaks were distorted.

5.3.2. Individual Determination of Pb(II), Cd(II), and Zn(II)

After the simultaneous detection of the metals, individual analyses were performed for comparison studies. The analyses were done according to the same parameters determined for the simultaneous experiments. Figures 5.3, 5.4, and 5.5 are the resulting voltammograms for 10-100 ppb metals. Figure 5.6 shows the resulting calibration plots. The E_{peak} values occur at the same potential for both determinations. This is one indication that no intermetallic species are formed. Table 5.1 lists the R^2 values and slopes for the calibration plots. These values are in good agreement with one another, suggesting also that no intermetallic species are formed. One issue observed during the course of the experiments was the broadening and misshaping of the Pb(II) peaks (individual analysis). The Pb(II) samples were the last in the set of experiments. Upon examination, the BiBE surface appeared dull with some black spots. This was a formation of bismuth oxide. A lifetime of the electrode would be estimated at 30 samples before a polishing step would be needed.

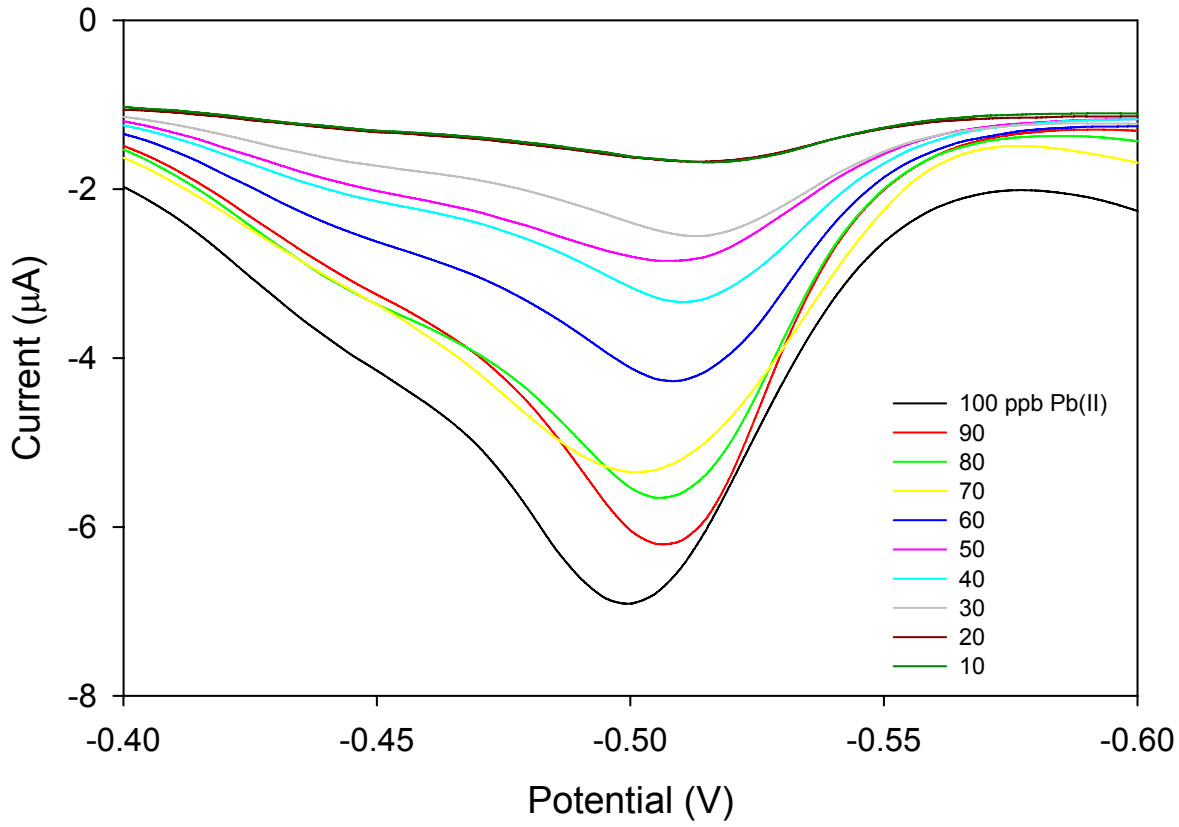

Figure 5.3. ASV calibration of Pb(II) detected at the BiBE. The concentration of Pb(II) solutions ranged from 10 to 100 ppb.

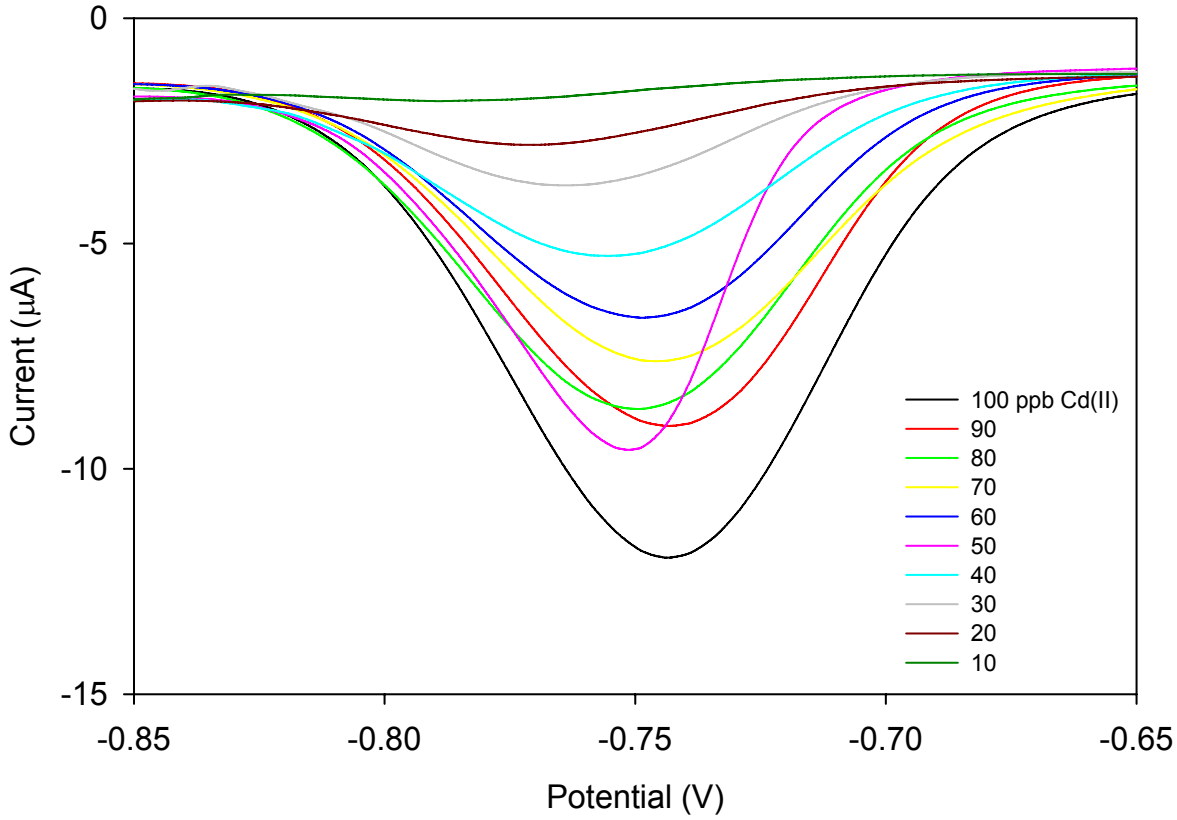

Figure 5.4. ASV calibration of Cd(II) detected at the BiBE. The concentration of Cd(II) solutions ranged from 10 to 100 ppb.

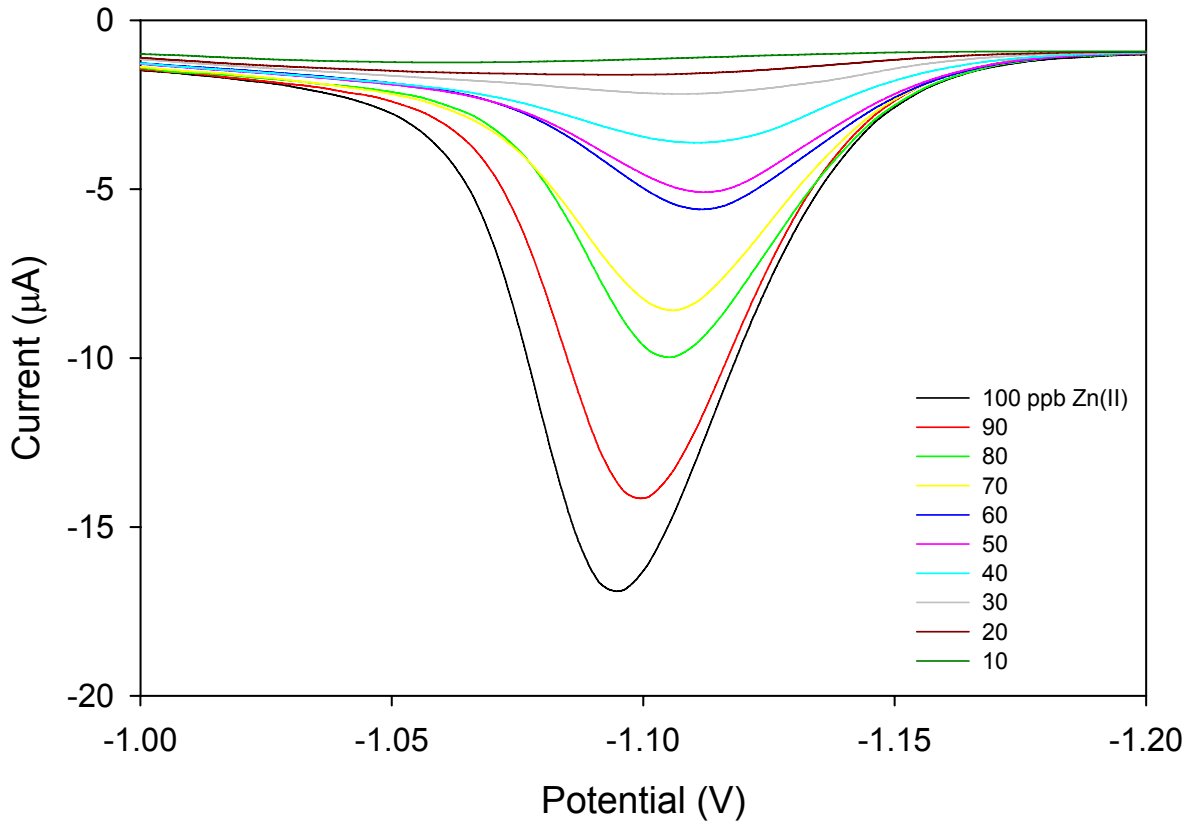

Figure 5.5. ASV calibration of Zn(II) detected at the BiBE. The concentration of Zn(II) solutions ranged from 10 to 100 ppb.

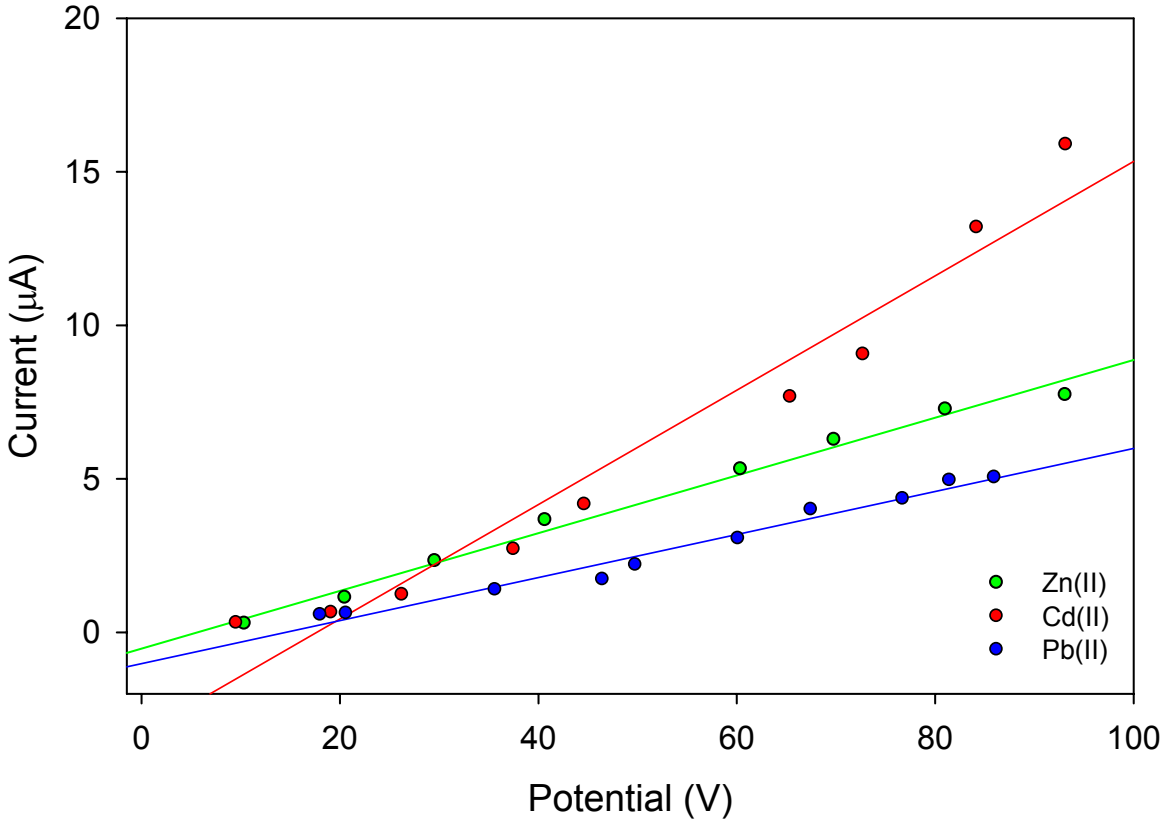

Figure 5.6. Calibration plots of Pb(II) (blue), Cd(II) (red), and Zn(II) (green) detected individually at the BiBE.

5.3.3. Difference in Electrode Surfaces between Experiments

Figures 5.7 and 5.8 are voltammograms of 10-100 ppb Pb(II), Cd(II), and Zn(II) at the 3 mm electrodes and the corresponding calibration plots, respectively. The currents are approximately four times larger, as expected, for the larger electrode. The R^2 values are also much better [0.989, Pb(II); 0.974, Cd(II); 0.984, Zn(II)]. The electrode was used for 20 samples. At that time, the electrode was left in open air until the next day when experiments were continued. A polishing step (described in Part 4), was used prior to the second set of experiments. Comparison of the slopes for the calibration plots are given in Table 5.2. The large difference in the slopes is most likely due to the difference in the electrode surface.

During the course of performing these experiments again, a power outage occurred. After this, the electrode formed a thick bismuth oxide layer (evident from a black layer on the electrode) after only three samples. It is believed the electrode was affected by the power outage. This was the only electrode with a 3 mm diameter, and due to time constrictions, all remaining experiments were performed with a 0.8 mm diameter electrode.

An electrode preservation study was done to determine the best way to keep the integrity of the electrode surface. It was found that leaving the electrode in water overnight, followed by a polishing step using the 0.05 mm alumina slurry on the Microcloth pad prior to the next set of experiments resulted in voltammograms on par with voltammograms collected before the storage period.

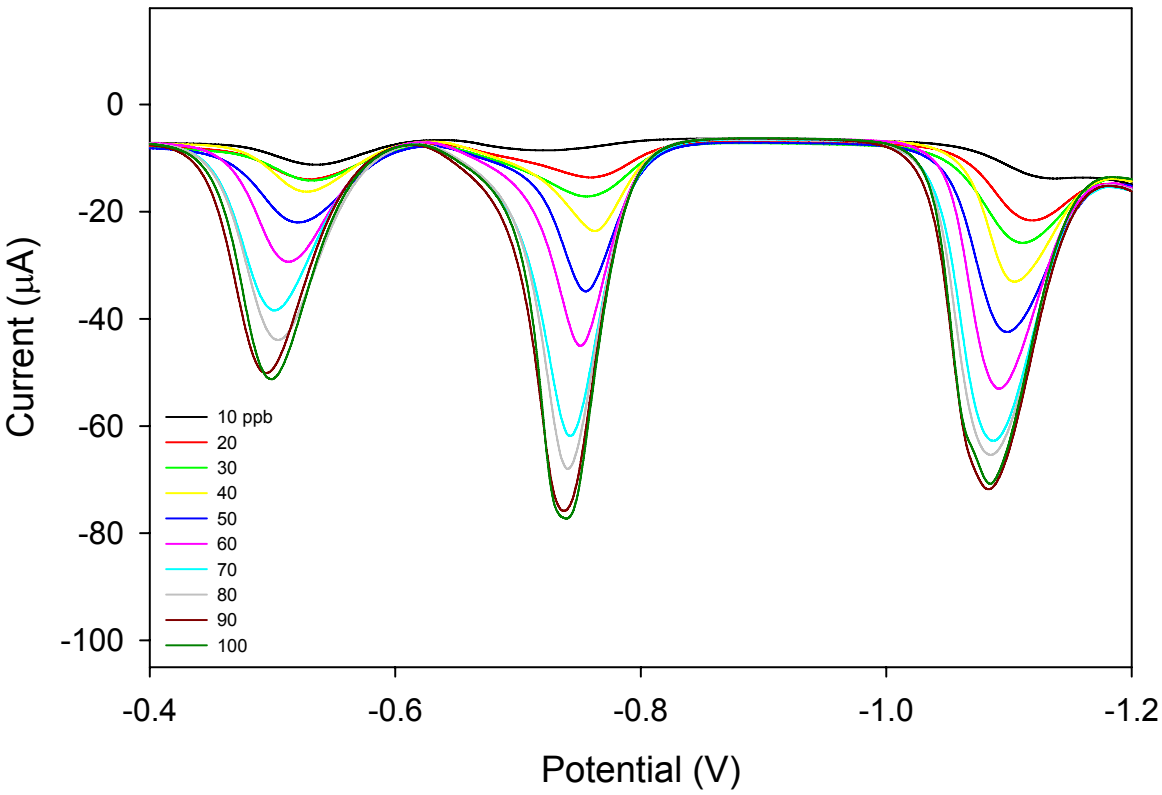

Figure 5.7. ASV of Pb(II), Cd(II), and Zn(II) detected simultaneously at the 3 mm BiBE. Standards ranged from 10 to 100 ppb.

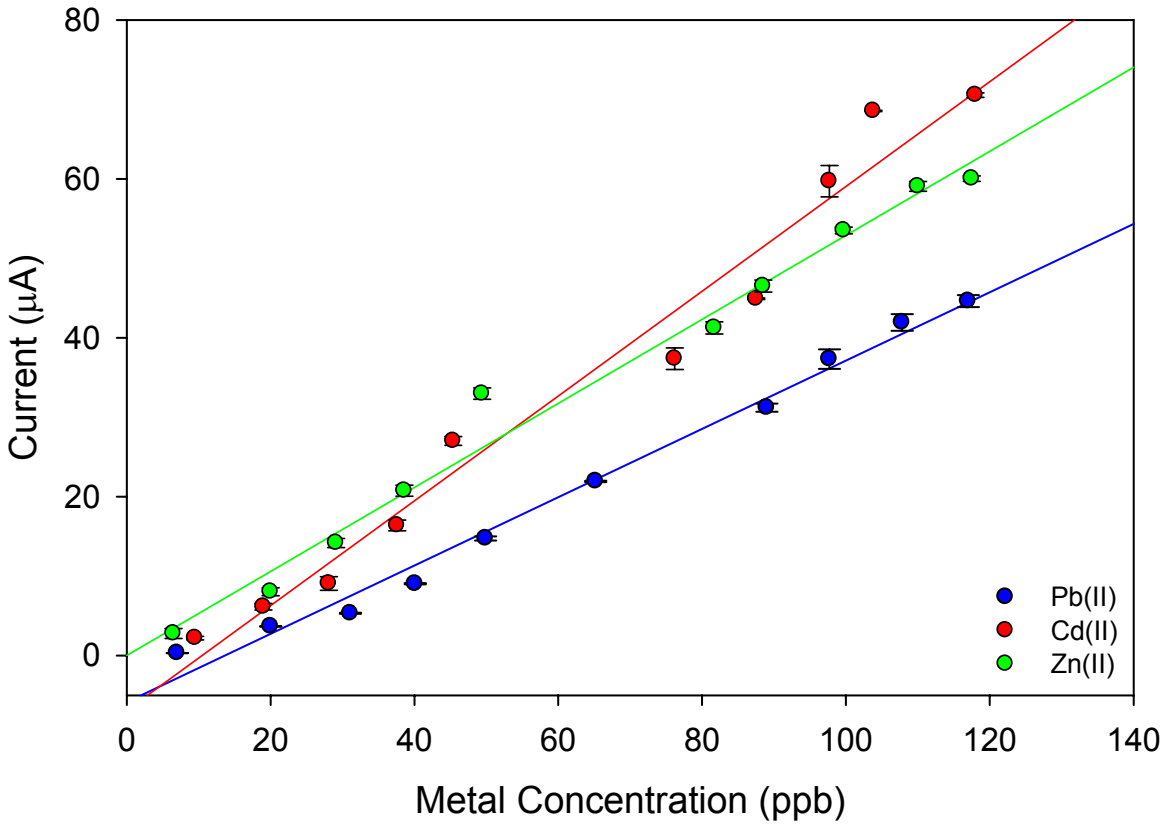

Figure 5.8. Calibration plot for simultaneous detection of Pb(II) (blue), Cd(II) (red), and Zn(II) (green) at the 3 mm BiBE.

Table 5.2. Slopes of the calibration plots for Pb(II), Cd(II), and Zn(II) detected simultaneously and individually at the 3 mm BiBE.

Metal	Slope (Simultaneous)	Slope (Individual)
Pb(II)	0.430	0.300
Cd(II)	0.659	0.473
Zn(II)	0.529	0.255

Table 5.3. Comparison of calibration plots for individual and simultaneous metal ASV detection (charge versus concentration).

Individual	R^2	**Slope**
Pb(II)	0.965	0.0057
Cd(II)	0.971	0.0098
Zn(II)	0.974	0.0080
Simultaneous	R^2	**Slope**
Pb(II)	0.981	0.0049
Cd(II)	0.973	0.0090
Zn(II)	0.993	0.0149

Calibrations were made for simultaneous and individual detection methods plotting the integration of the peaks (charge) versus concentration. These calibrations yielded better R^2 values, but the slopes of the metals determined simultaneously were different from those determined individually. These values are listed in Table 5.3. This is most likely a result of the peak distortion seen in the individual metal analysis from the formation of the bismuth oxide layer.

5.3.4. Dynamic Range and Detection Limits

The limit of detection calculated for each metal (3σ) is 105 ppt for Pb(II), 54 ppt for Cd(II), and 396 ppt for Zn(II) for the 3 mm diameter electrode. These values are for a 180 s accumulation time and were calculated from the standard deviation of the mean of 3 measurements of the background current. The dynamic range for both electrodes was 10-100 ppb for all metals.

5.3.5. Analytical Application

The 0.8 mm diameter BiBE was used to determine the Pb(II), Cd(II), and Zn(II) levels in a sample from the Tennessee River. Sodium acetate was added to a 20-mL river water sample to a final concentration of 0.1 M. The pH was then adjusted to 6.0 with acetic acid. After a 240 s accumulation period, SWV was used stripping analysis as described above. The results showed no peaks corresponding to Pb(II), Cd(II), or Zn(II). Therefore, it was determined that the concentrations of these metals in the sample are negligible.

5.4. CONCLUDING REMARKS

The BiBE has been shown as a useful electrode for the determination of metal species in environmental water samples. Detection limits in the low ppt range are comparable to those of the BiFE and other electrodes. These qualities demonstrate that the BiBE promising as an environmental sensor.

REFERENCES

(1) Bard, A. J.; Faulkner, L. R. *Electrochemical Methods: Fundamentals and Applications*, 2nd ed.; Wiley: New York, 2001.

(2) Jorge, E. O.; Neto, M. M. M.; Rocha, M. M. *Talanta* **2007**, *72*, 1392-1399.

(3) de Carvalho, L. M.; do Nasciniento, P. E.; Koschinsky, A.; Bau, M.; Stefanello, R. F.; Spengler, C.; Bohrer, D.; Jost, C. *Electroanal.* **2007**, *19*, 1719-1726.

(4) Hutton, E. A.; Hocevar, S. B.; Mauko, L.; Ogorevc, B. *Anal. Chim. Acta* **2006**, *580*, 244-250.

(5) Prior, C.; Walker, G. S. *Electroanal.* **2006**, *18*, 823-829.

(6) Svancara, I.; Baldrianova, L.; Tesarova, E.; Hocevar, S. B.; Elsuccary, S. A. A.; Economou, A.; Sotiropoulos, S.; Ogorevc, B.; Vytras, K. *Electroanal.* **2006**, *18*, 177-185.

(7) Song, Y.; Swain, G. M. *Anal. Chim. Acta* **2007**, *593*, 7-12.

(8) El Tall, O.; Jaffrezic-Renault, N.; Sigaud, M.; Vittori, O. *Electroanal.* **2007**, *19*, 1152-1159.

(9) Kachoosangi, R. T.; Banks, C. E.; Ji, X. B.; Compton, R. G. *Anal. Sci.* **2007**, *23*, 283-289.

(10) Hutton, E. A.; van Elteren, J. T.; Ogorevc, B.; Smyth, M. R. *Talanta* **2004**, *63*, 849-855.

(11) Pauliukaite, R.; Hocevar, S. B.; Ogorevc, B.; Wang, J. *Electroanal.* **2004**, *16*, 719-723.

VITA

Kristie Carter Armstrong was born in Jackson, Mississippi on July 16, 1977. Her family moved around Texas and Mississippi, but settled in Brandon, Mississippi. Kristie graduated from Brandon High School in 1995. She attended Hinds Community College in Pearl, Mississippi, where she earned her Associate of Arts degree in Chemistry in May 1997. Upon graduation from Hinds, Kristie transferred to the University of Southern Mississippi in Hattiesburg. After only one semester, she decided to transfer to Mississippi State University in Starkville. During her studies at MSU, she participated in undergraduate research under the instruction of Dr. Charles S. Henry. She also participated in the cooperative study program and worked for three semesters as a laboratory technician at Akzo Nobel, Eka Chemicals in Columbus, Mississippi. In May 2001, Kristie graduated with her Bachelor of Science degree with a major in chemistry. Before deciding on attending graduate school, Kristie worked as a Research Assistant in the Orthopedic Surgery department at the University of Mississippi Medical Center in Jackson. After only one semester, it became apparent that she wanted to pursue an advanced degree. In Spring 2002, Kristie joined the research group of Dr. S. Douglass Gilman and began taking graduate courses in the chemistry department at the University of Tennessee in Knoxville. After two years, Dr. Gilman left UT. At that time, Kristie joined the analytical subgroup of Dr. Ziling (Ben) Xue. She completed her requirements for the Ph.D. program at UT in Fall 2007. Kristie has presented her research at meetings including the American

Chemical Society Nation Meeting, the Southeastern Regional Meeting of the American Chemical Society, and the Pittsburg Conference. She also held positions of Treasurer and Younger Chemist Committee Chair in the Association of Chemistry Graduate Students.